ANALYSIS OF FORECAST PERFORMANCE FOR HIT, MISS, AND FALSE

ALARM THUNDERSNOW EVENTS DURING *ROCS*

A Thesis Presented to the Faculty of the Graduate School at the University of

Missouri

In Partial Fulfillment of the Requirements for the Degree Masters of Science

by

KATIE CRANDALL

Dr. Patrick Market, Thesis Advisor

MAY 2010

The undersigned, appointed by the dean of the Graduate School, have examined

the thesis entitled

ANAYLYSIS OF FORECAST PERFORMANCE FOR HIT, MISS, AND

FALSE ALARM THUNDERSNOW EVENTS DURING *ROCS*

Presented by Katie Crandall,

a candidate for the degree of master of science,

and hereby certify that, in their opinion, it is worthy of acceptance.

_____

Associate Professor Patrick Market

_____

Professor Anthony Lupo

_____

Professor Bruce Cutter

ACKNOWLEDGEMENTS

Table of Contents

Figures

xv

Tables

Abstract

Thundersnow (TSSN) is a mesoscale event that is typically associated with large amounts of precipitation and both in-cloud and cloud-to-ground lightning. Starting in 2003, the Research on Convective Snows (*ROCS*) group began issuing TSSN outlooks each day during the cold season for areas of the U.S. located between the Rocky and Appalachian mountains. The purpose of the outlooks was to inform users on whether TSSN should be expected in the central U.S. during the ensuing 24-hour period and for what location, if applicable. The issuance of daily outlooks continued for five seasons from 2003 through 2008. Three potential TSSN events along with their issued outlooks from the 2003 to 2008 time period were chosen for further investigation. These events fell in the category of being a "hit," "false alarm," or "missed," forecast. The purpose of this investigation is to better understand the reasons for the creation of either a successful TSSN forecast or an unsuccessful TSSN forecast. Also, a verification of all TSSN outlooks for that five-year period was performed to determine if forecasting skill was improving as time progressed.

Chapter 1   Introduction

Thundersnow (TSSN) is a mesoscale event that is typically associated with large amounts of precipitation and both in-cloud and cloud-to-ground lightning. Most TSSN activity for the United States occurs between the months of October and March with March being the most active month. TSSN is often observed in the northwest and northeast sectors of dynamic mid-latitude cyclones (Market et al. 2002). Research has also shown that TSSN events tend to occur with storm total snowfall greater than 15 cm making them an important feature to understand from a forecasting perspective (Crowe et al. 2006).

Starting in 2003, the Research on Convective Snows (*ROCS*) group began issuing TSSN outlooks each day during the cold season for the area of the United States pictured in Figure 1.1. The outlooks were issued at 1800 UTC and expired at 1800 UTC the following day. The purpose of the outlooks was to inform users on whether TSSN should be expected in the central U.S. during the ensuing 24-hour period and for what location, if applicable. The issuance of daily outlooks continued for five seasons from 2003 through 2008. Although these TSSN outlooks had been issued for some time, there has never been any significant verification performed on these forecasts. This thesis work is the first attempt at verification and analysis of TSSN forecasts issued by the *ROCS* group.

NO CONVECTIVE SNOW OUTLOOK
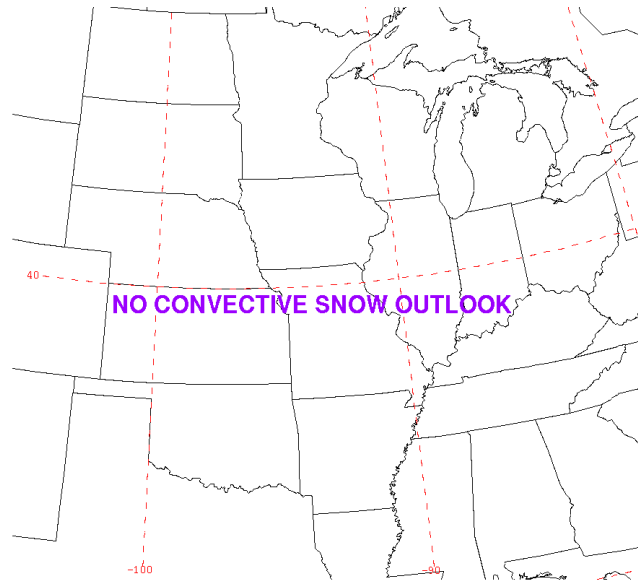
Figure 1.1 Indicates the region for which the *ROCS* group created convective snow outlooks

1.1   Purpose

The purpose of this research is to better understand the forecasting of TSSN, and to perform verification on the forecasts issued by the *ROCS* group between 2003 and 2008. Through verification it can be determined whether there was improvement in the forecasting of TSSN and where there may still be problems in the forecasting process. This verification may then help operational forecasters create more accurate TSSN forecasts. We also hope to determine common issue(s) that may have affected the outcome of each forecast.

1.2 Objectives

To achieve the purpose previously mentioned, the following objectives are identified:

- Create verification statistics on all forecasts issued by the *ROCS* group between 2003 and 2008.

- Analyzed selected 24-hour forecasts issued by the *ROCS* group. One forecast shall include a "hit" event, one forecast shall include a "false alarm" event, and one forecast shall include a "missed event."

- Complete case studies on all three chosen forecast events, particularly focusing on moisture, lift, and stability profiles.

Chapter 2   Literature Review

In order to complete the objectives of this research, an extensive literature review has been performed in order to understand the causes of and the ingredients necessary for TSSN as well as identify the verification statistics that need to be performed on the *ROCS* forecasts.

2.1   TSSN Climatology & Composites

Market et al. (2002) used data from 1961 through 1990 to create a climatology of TSSN events spanning the continental United States. For the climatology, surface data from 204 stations were used to identify TSSN events. Only 3-hour synoptic observations were used for the climatology. From the collected synoptic observations, TSSN events were identified by observations that contained snow with reports of lightning in the vicinity. An event was distinguished from another event by spacing and time. If 6-hours passed between observations of TSSN and or there was a distance greater than 1100 km between TSSN observations, then the observations are categorized as separate events.

From the analysis of the identified events it was discovered that March is the preferred month for TSSN events. However, Midwestern TSSN events can occur from October through April. Most TSSN events occur in eastern Nevada and Utah, the Central Plains states, and the Great Lake states. It has been found that most TSSN events have short time durations, are associated with light to moderate snowfall, and often cover

small areas. From the data used by Market et al. (2002), there is no clear diurnal preference.

Some other findings from the data are that most TSSN events are associated with dynamic mid-latitude cyclones, are located an average of 440 km from the mid-latitude cyclone's center, and tend to occur in the northwest or northeast sectors of the mid-latitude cyclone. Finally, most events are associated with overcast skies, average surface temperatures around 30°F, average dewpoints only a few degrees cooler, and northerly winds that average 16 kts.

Market et al. (2004) scrutinized TSSN events from 1961 through 1990 and then separated out the events that occurred in the Midwestern United States. 97 events were identified as occurring in the Midwestern United States. Those 97 events were then separated into groups depending upon the setup of each event. Events that were associated with mid-latitude cyclones (80 cases total) were used for further examination and put through a composite process.

Analysis for Market et al. (2004) was done by generating mean fields of the standard atmospheric variables at the levels of 900-mb, 850-mb, 700-mb, 500-mb, and 300-mb. The fields were generated for the time of event initiation and at hours 12, 24, 36, and 48 before event initiation. The composites were generated for locations centered on the TSSN events.

From the composites of the TSSN events, it was shown that TSSN that occurred to the northwest of the center of the mid-latitude cyclone often occurred with better-developed, deeper, and more negatively tilted mid-latitude cyclones compared to mid-latitude cyclones with events that occur to the northeast of the mid-latitude cyclone. It

appears that events that occur to the northeast develop in systems that are still evolving. Out of the 80 classified events analyzed, 33 occurred to the northwest of the mid-latitude cyclone, while 19 occurred to the northeast of the mid-latitude cyclone. The other 28 events associated with a mid-latitude cyclone occurred in some other quadrant of the mid-latitude cyclone.

2.2   TSSN & Heavy Precipitation

It has been generally assumed that TSSN is associated with heavy snowfall. However, there was no significant research to support this assumption. Crowe et al. (2006) studied the correlation between TSSN and significant snowfall within a 24-hour period. Observations from major airports in the upper Midwestern states from the years 1961-1990, which were used by Market et al. (2002) to identify TSSN events, were reused here. Those TSSN events were then compared to snowfall totals from cooperative climate observer stations that were located near the observations.

From the analysis of the events and the snowfall totals, it was determined that TSSN most often occurs in close proximity to areas with snowfall greater than 15 cm. However, TSSN only accompanied the greatest snowfall in 1 out of every 3 storms investigated (Crowe et al. (2006)). It was also determined that the presence of TSSN often indicates that the storm it is associated with are Midwestern mid-latitude cyclones likely to produce significant snowfall at some point and some location in their life cycles.

2.3 TSSN Development

According to Johns and Doswell (1992) the three ingredients necessary for deep, moist convection are moisture, lift, and instability. In a similar fashion Nicosia and Grumm (1998) demonstrated from past and current research that the main contributors to mesoscale banding, which are often co-located with TSSN, are adequate moisture, frontogenesis (which provides a lifting mechanism) and conditional symmetric instability (CSI). Moisture content of the atmosphere is an easily understood concept but frontogenesis and instability are more difficult concepts to grasp, so we shall examine them more closely at this junction.

2.3.1 Frontogenesis

Frontogenesis is the term used to describe the strengthening of a frontal zone. Mathematically frontogenesis is defined as:

$$F = \frac{1}{|\nabla_p \theta|} \left[-\left(\frac{\partial \theta}{\partial x}\right)^2 \frac{\partial u}{\partial x} - \frac{\partial \theta}{\partial y}\frac{\partial \theta}{\partial x}\frac{\partial v}{\partial x} - \frac{\partial \theta}{\partial x}\frac{\partial \theta}{\partial y}\frac{\partial u}{\partial y} - \left(\frac{\partial \theta}{\partial y}\right)^2 \frac{\partial v}{\partial y} \right] \tag{1}$$

This is the two-dimensional scalar frontogenetic equation expanded from the original equation in Pettersen (1956) by Nicosia and Grumm (1998). This equation is defined as the Lagrangian rate of change of the magnitude of the horizontal potential temperature gradient due to the horizontal wind. In practice, when there is an increase in the potential temperature gradient then frontogenesis is considered to be occurring.
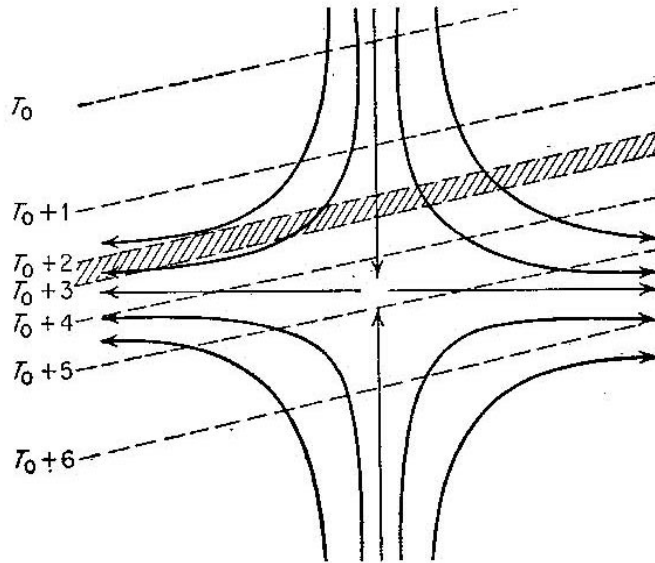
Figure 2.1 Diagram from Petterssen (1956). The diagram shows frontogenesis through a kinematic diagram. The hatched area is the line of frontogenesis and it moves toward the axis of dilatation (horizontal centerline) as the temperature gradient tightens. This diagram is also an example of pure deformation. The dashed lines are isotherms and the solid lines are isobars.
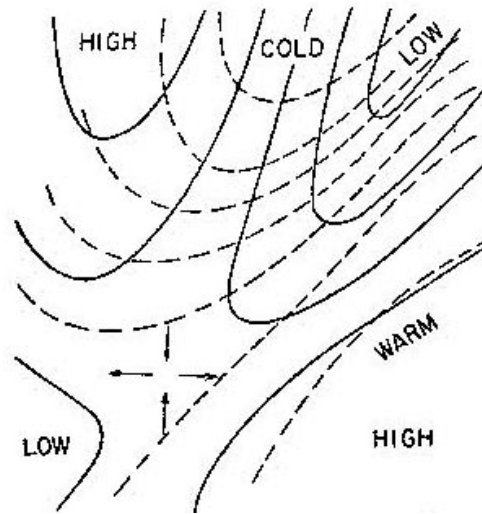
Figure 2.2 Diagram from Petterssen (1956). The diagram is a typical frontogenetical field seen in the real atmosphere. The col point is located where the converging and diverging arrows are located in the diagram. The dashed lines are isotherms and the solid lines are isobars.

The original equation from Pettersen (1956) is defined as:

$$F = \frac{d}{dt}[\boldsymbol{\nabla}\theta] \tag{2}$$

Frontogenesis can usually be identified in the atmosphere by detecting horizontal deformation (Figs. 2.1 and 2.2). According to Banacos (2003), horizontal deformation located between 850-mb and 500-mb and a defined deformation zone located around 700- mb is the most conducive synoptic setup for heavy banded precipitation. There will also be col point(s) between 850-mb and 500-mb. Forecasters should look for deformation inside a mid-latitude cyclone or a frontal zone with strong vertical wind shear and strong horizontal winds. This is a location that is inclined to strong frontogenetic forcing that has the ability for the production of heavy precipitation. However, forecasters must be aware that col point(s) located aloft do not automatically indicate that mesoscale banding will occur. When col point(s) aloft are identified in gridded soundings a forecaster should be aware of the potential for mesoscale banding and monitor real time observations, frontogenesis fields, and storm-relative winds for the possibility of banding.

2.3.2 Symmetric Instability

CSI is a more difficult quantity to identify and use compared to frontogenesis. To understand CSI, it is important to understand other types of instability and to identify how CSI was first investigated by the meteorological community. Indeed, Schultz et al.

9

(2000) examine the history and use of the terminology of conditional instability (CI), potential instability (PI), and CSI.

According to Schultz et al. (2000), Rossby (1932) was the first to coin the term "CI" as the definition of instability with environmental lapse rates between the dry-adiabatic and moist-adiabatic lapse rates. Sherwood (2000) showed that CI is commonly used with the above definition (lapse-rate definition) as well as the available-potential energy definition (a parcel in the atmosphere that contains positive buoyant energy).

Sherwood (2000) takes a closer look at CI and the misconceptions that have been associated with it. CI is usually identified when the environmental lapse rate is steeper than a moist-adiabat but is less steep than a dry-adiabat. This is the most accepted definition, but there is also a more recent definition that defines CI as a condition in which a parcel of ascending air can become positively buoyant. In the atmospheric community there has been some confusion between these two definitions that needs to be resolved.

The most common definition of CI is the lapse-rate definition. The problem with this definition is that it is associating CI with actual instability, which is not accurate. The lapse-rate definition indicates more of an uncertainty for convection. It helps a forecaster to narrow down areas in the atmosphere where convection may occur and examine them closer.

The other definition for CI came about from the fact that low-level air parcels that are lifted high enough in the atmosphere will become positively buoyant. Forecasters will often use convective available potential energy (CAPE) to determine the amount of instability that may be released if parcels are adequately lifted. Both definitions of CI are

useful in the forecasting process, but it is important to understand what each definition is implying when trying to identify areas of CI.

The lapse-rate definition of CI cannot determine unambiguous parcel stability, so the term PI was developed. According to Schultz et al. (2000), Hewson (1937) developed the term PI to describe the process of a layer of the atmosphere being lifted during ascent over a front. This type of instability offers a way to distinguish large-scale convection from isolated convection. PI is often identified in areas where deep, moist convection is likely to occur, even if the initiation of the convection is not from a layer being lifted over a front. It must be realized that not all "convective" atmospheric environments have the presence of PI.

Another section of the Schultz et al. (2000) paper shows how ingredients-based methodologies' use of the term instability is supposed to refer to the lapse-rate definition of CI. Even though, there are inherent problems with the lapse-rate definition's use in the ingredients-based methodology, it is still useful to forecasters because it separates moisture from lapse rates. Finally, the 2000 paper discuses the diagnosis of CSI. CSI can be diagnosed using either its lapse-rate definition or its available-energy definition. The lapse-rate definition of CSI is the same as the relationship of θ_{es} to geostrophic absolute momentum (M_g) or the use of negative saturated geostrophic potential vorticity ($MPV_g{}^*$). The available-energy definition is the same as the use of slantwise convective available potential energy (SCAPE).

Besides the discussion of the terminology and history of different types of instability, what must also be taken from the Schultz et al. (2000) paper is that focusing on instability in the atmosphere should not keep forecasters and researchers from zeroing

in on the real issue. That issue is, "what is the lifting mechanism for the clouds and precipitation?" This is the most important part of the forecasting process because the degree of instability (either derived from the lapse-rate definition or available-potential energy definition) only determines the response to the forcing mechanism.

CSI is often used as an explanation for banded precipitation and clouds, but according to Schultz and Schumacher (1999), CSI may be overly used and misused by forecasters. They identified four reasons why CSI was not being used correctly by forecasters and researchers:

- The use of CSI has certain limits and restrictions that are not always understood or are ignored by researchers and forecasters.

- Advances in satellite imagery and Doppler radar have made identification of banded precipitation and clouds easier thus needing an explanation for the bands.

- With the advent of gridded numerical-models more researchers and forecasters have the ability to model environments with CSI and evaluate CSI in operational situations.

- Model output data of CSI and observed CSI don't always correlate which makes it difficult to correctly understand the occurrence of CSI in the real atmosphere.

One of the purposes of the 1999 paper was to help the atmospheric science community understand the difference between CSI and slantwise convection and how they are connected. CSI and slantwise convection are not interchangeable. First we must understand the formation of slantwise convection. Like moist gravitational convection: moisture, lift, and instability must all be present for slantwise convection to occur. This

is why CSI and slantwise convection are not the same thing. CSI is one of three ingredients needed for slantwise convection.

Following Schultz and Schumacher (1999), when diagnosing CSI, meteorologists should use the basic state of saturated equivalent potential temperature $\bar{\theta}_{es}$ and M_g for the analyses. However, it is permitable to use just θ_{es} for diagnosing CSI but not absolute momentum (M). θ_{es} can be substituted for $\bar{\theta}_{es}$ because the atmosphere is hydrostatic to a decent approximation and using θ_{es} instead of $\bar{\theta}_{es}$ introduces only a very small error. On the other hand M cannot be substituted for M_g because specific cases where strong cyclonic shear is present may appear more "inertially" stable along a basic state potential temperature $(\bar{\theta})$ surface then they actually are. When diagnosing potential symmetric instability (PSI) instead of CSI, θ_e should be used and not θ_{es} because the assumption is that the atmosphere is not saturated. However, on that note, if the assumption is that the atmosphere is saturated, then when determining locations of CSI it is permitable to use θ_e instead of θ_{es}.

There is another method of identifying CSI in the atmosphere without using θ_e and M_g in a cross-section. Moore and Lambert (1993) show that regions of CSI can be quickly and easily measure using equivalent potential vorticity (EPV) compared to the conventional method of using M_g and θ_e.

Cold season extratropical cyclones can sometimes have mesoscale bands of precipitation embedded within the cyclone's areas of precipitation. These bands can result from various processes including CSI. The presence of CSI may result in slantwise convection which often can organize precipitation into bands embedded in areas of lighter precipitation. CSI in near-saturated environments (greater than 80% relative

13
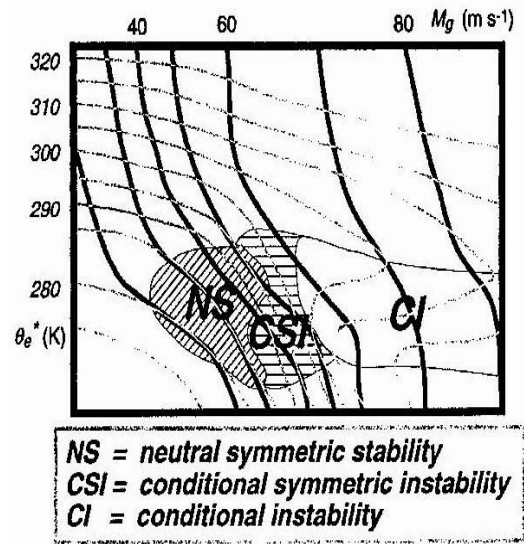
Figure 2.3 An unpublished figure from James Moore and Sean Nolan which was adopted by Schultz and Schumacher (1999) depicting the location of CSI in a cross-section of the atmosphere near a frontal zone. The thick black lines are M_g and the thin gray lines are θ_e. Contours depict typical values.

humidity) can be assessed by cross sections taken normal to the midtropospheric thermal wind and by plotting M_g and θ_e. Regions of CSI are then determined by comparing the slope of the θ_e surfaces with the slope of the M_g surfaces. CSI would be present in regions where the θ_e surfaces are more vertical then the M_g surfaces, but do not overturn as in the cases of CI (Fig. 2.3).

14

EPV can be used to help determine regions of CSI in a saturated atmosphere. The equation from Moore and Lambert (1993) for EPV is:

$$EPV = g\left[\left(\frac{\partial M_g}{\partial p}\frac{\partial \theta_e}{\partial x}\right) - \left(\frac{\partial M_g}{\partial x}\frac{\partial \theta_e}{\partial p}\right)\right] \tag{3}$$

$$\quad\quad\quad\quad A \quad B \quad\quad\quad C \quad D$$

Where $g = 9.806\ ms^{-2}$ and p stands for atmospheric pressure. Term A shows the change in absolute geostrophic momentum with respect to pressure. Term A is usually negative in levels below the jet stream because $M_g = V_g + fx$, where f represents the Coriolis parameter and V_g is the geostrophic wind component normal to the cross-section. This equation indicates that M_g is directly proportional to V_g. In typical atmospheric conditions V_g increases with height as pressure decreases up to the jet stream. Under these conditions term A is negative. If vertical wind shear increases, due to increasing V_g with height, term A will become more negative and M_g surfaces become more horizontal. In the location of frontal zones this lends itself to greater chances for CSI because in these regions θ_e surfaces are already steep (more vertical).

Term B is usually positive due to the definition of M_g, that indicates that a cross-section of the atmosphere must be taken normal to the geostrophic wind. This also indicates that the cross-section is normal to the thermal wind. With the positive x-direction in this cross-section pointing toward warmer air, θ_e surfaces slope down causing term B to be positive. When term A and term B are multiplied, the final result is

15

negative, and will become more negative with stronger vertical wind shear or a stronger θ_e gradient. This final result we will call term 1.

Term C is usually positive. The reason for this brings us back to the equation $M_g = V_g + fx$. In this environment, $\frac{\partial M_g}{\partial x}$ is the absolute geostrophic vorticity. In the Northern Hemisphere absolute vorticity is usually positive, so in most cases term C will be positive.

Term D is the term that is dependent upon the potential stability profile of the atmosphere. If term D is positive, then the atmosphere is potentially unstable. If term D is equal to zero, then the atmosphere is potentially neutral. Finally, if term D is negative, then the atmosphere is potentially stable. Now EPV can be evaluated by subtracting term 1 from term 2. As said earlier, term 1 is usually negative so term 2 must be determined. There are now three possibilities for the value of EPV due to term D affecting the outcome of term 2.

The first possibility is that term D is positive. This will make term 1 minus term 2 negative, thus making EPV negative. If this occurs then the atmosphere is potentially unstable. If there is plentiful moisture and a source of lift, then upright convection will occur. Following Schultz and Schumacher (1999) the moist atmosphere can release both CSI and CI, but upright convection occurs faster and will dominate over slantwise convection.

Returning to Moore and Lambert (1993) the second possibility is that D is equal to zero. This will make term 2 equal zero and that will not affect the value of EPV. Term 1 minus term 2 would then be a negative value, making EPV negative.

16

The last possibility is that D is negative. This will make term 2 negative. When term 2 is subtracted from term 1, the result is a greater value of EPV, not necessarily positive but it will make PSI less likely to occur.

To summarize if EPV in a region is < 0 and the surrounding atmosphere is potentially stable then this would indicate PSI as long as absolute vorticity is negative on a θ_e surface. If EPV > 0 the atmosphere is symmetrically stable. As mentioned above PSI and potential instability can occur in the same region. This is why it is important to look at both EPV terms when diagnosing PSI.

Returning to the Schultz and Schumacher (1999), it is argued that when diagnosing CSI, meteorologists must be aware of other factors that can cause slantwise convection or banded precipitation and clouds besides CSI. If it is determined that the atmosphere is stable with respect to moist slantwise convection or moist gravitational convection, banded precipitation and banded clouds may develop from forced ascent due to orographic lift or frontogenesis. Also, when frontogenesis and CSI are both present with the development of banded precipitation and clouds, it is not correct to separate CSI circulations from frontal circulations.

The Schultz and Schumacher (1999) paper also gives meteorologists some insight on things they will discover when diagnosing CSI and some notions about CSI diagnoses that are not always correct. When diagnosing CSI, areas of CI as well as inertial instability may be identified during the process instead of CSI. Also, when CSI and PSI exist in the same region or when CI and PI exist in the same region along with ample moisture and lift, then a conglomeration of moist gravitational convection and moist slantwise convection may occur due to the release of convective-symmetric instability. If

lightning, strong downdrafts, intense precipitation, and/or deep cumulonimbus are present they do not automatically indicate the presence of moist gravitational convection compared to moist slantwise convection. Another important concept is that banded precipitation and clouds may only be weakly related to the measures of CSI. Although, when it is suspected that banding may be due to CSI, parameters such as orientation, spacing, and movement of the bands should be analyzed in greater detail. Finally, today's mesoscale and operational forecast models do not adequately identify separate CSI circulations, so they should be used with caution to forecast or diagnose CSI.

2.3.3 Potential Instability (PI)

Market et al. (2006) helped to establish how a typical atmospheric sounding accompanying TSSN would appear. Soundings are useful in TSSN cases because they help to determine if the three ingredients (moisture, lift, and instability) are present for moist convection. In the paper, two sets of soundings are compared. The first set of soundings included ones that were launched close to the location and time of active TSSN. The second set of soundings is similar to the first set on a synoptic scale, but there is no lighting near the sounding locations. Both sets of soundings are associated with extratropical low pressure systems that have at least two closed isobars on a 4 mb pressure map. Soundings were only selected if they occurred between the Rocky Mountains and the Appalachian Mountains and were not influenced by bodies of water. Finally all TSSN soundings were taken between the dates of 1961 and 1990.

When the two sets of soundings were compared, the conclusions that were drawn were that the set of soundings associated with TSSN were located in environments that

were less stable and more conducive lightning production than the set not associated with TSSN. Also, with the information from the comparison a composite sounding for TSSN was developed. The typical TSSN sounding will have a nearly moist neutral environment located above the frontal inversion, the most unstable layer in the sounding will be located around 30 to 50 mb above the layer of the inversion, the sounding will be cold enough through all layers for snow production, and there will also be increased drying within 100 mb of the level in which the most unstable parcel was lifted.

2.4 Lightning Development in Banded Snow

Market and Becker (2009) looked at frequency and other issues of lighting associated with snowfall during the winter months of the central United States. Data for this paper were taken from two different sources. The lightning data came from the National Lightning Detection Network (NLDN) and data for snowfall intensity came from Level III radar base reflectivity created on the Doppler (WSR-88D) radar network. Radar scans occurred around every 6 minutes, and then lightning strikes where matched to each time period. After collecting the radar and lightning data animated loops of radar base reflectivity in precipitation mode were reviewed to discern snowfall banding. Upon completion of this phase, 4 categories were developed to show were each lightning flash was located in correlation to the snowfall band. The 4 categories were leading edge, trailing edge, core, and not correlated.

24 cases of banded snowfall in the central United States and 1088 flashes of lightning were analyzed for the paper. The cases primarily came from the years 2004-2005 and 2005-2006 and the winter months of October through April. From the analysis

it was discovered that negative lightning flashes were much more common than positive lightning flashes for these 24 cases. Most research up until this paper generally concluded that positive lighting strikes were more common in convective snow. A reason for this may be that most of the research on snowfall and lightning was done in Japan and was associated with maritime or coastal weather patterns compared to continental weather patterns. This research also determined that lightning flashes may occur at the same time as the highest radar reflectivities, but a 1:1 correlation only occurred in the their data set 6% of the time. However, it was found that the mean distance from the average lightning flash to the highest reflectivity in a radar snow band is 17 km. For the median, it is 9 km. This indicates that lightning is often found near the area of the greatest immediate snowfall.

Van den Broeke et al. (2005) created guidelines for lightning development in convective lines with low-instability and strong forcing. Since TSSN tends to develop in similar environments, these guidelines can be applied to lightning development that occurs with snowfall.

For lightning to develop in environments with low-instability and strong forcing there must at least be sufficient CAPE to support upward vertical motions exceeding 6-7 ms^{-1} within the lower mixed layer of the cloud. This region is approximately between -10° C and -20° C. Lifted Condensation Levels (LCLs) should be warmer than -10° C and Equilibrium Levels (ELs) should be colder than -20° C. Of course these are only guidelines and an event may not conform to all of them.

2.5   Forecast Verification

In Chapter 7 of Wilks's (2006) book *Statistical Methods in the Atmospheric Sciences*, forecast verification is discussed in detail and how it is applied to the field of meteorology. Forecast verification is used as a means to evaluate the accuracy of forecasts. Forecast verification is most often used in meteorology, but can be applied to many other fields. There are numerous forecast verification methods that are used to verify different aspects of a forecast.

Forecast quality is often analyzed using specific scalar attributes. Some of the most common scalar attributes used in forecast verification is presented in Chapter 7.1.3 of Wilks's book. Accuracy of a forecast is the measure of the correlation between a particular forecast and the observations of the forecasted event. Accuracy as a scalar attribute is used to summarize the quality of the forecast using only one number. Bias, systemic bias, or unconditional bias are all terms that refer to the correlation between the average forecast for an event and the average observation of the forecasted event. An example of a bias would be forecasts that overestimate rain consistently for a particular type of event. Reliability, conditional bias, or calibration are all terms that refer to the connection between the forecast and the average observation for certain values in the forecast. Resolution is the degree that the forecasts separate the observed events into groups. Discrimination is the exact opposite of resolution in that it is the differences between the conditional averages of the created forecasts for different values of the actual observations. Finally, sharpness or refinement refers to only the forecast and not the actual observations.

Forecast skill is the measurement of the relative accuracy of a group of forecasts with reference to a control.

$$SS_{ref} = \frac{A - A_{ref}}{A_{perf} - A_{ref}} \times 100\% \qquad (4)$$

Where A is a measure of accuracy, A_{ref} is the accuracy of the reference forecast, and A_{perf} is the measure of accuracy from a perfect forecast.

If $A = A_{perf}$ then the final skill score is 100%. If $A = A_{ref}$ then the final skill score is 0%, which means that the forecast is no better than the reference forecast. If $A < A_{ref}$ then the final skill score is less than 0%, which means that the forecast is worse than the reference forecast.

The 2×2 (Table 2-1) contingency table is often used in forecast verification and is usually a one-to-one correlation between nonprobabilistic forecast values and the discrete predictand values that they correspond to.

For the verification of the $ROCS$ forecasts, the most important formula from chapter 7 of the Wilks book is the threat score (TS) or otherwise known as the critical success index:

$$Critical\ Success\ Index = TS = \frac{A}{A + B + C} \qquad (5)$$

Although the terms "threat score (TS)" and "critical success index" are interchangeable, to lessen confusion, the term "threat score (TS)" will be used from now on. The TS is the total number of "hit" forecasts divided by the total number of "hit"

		Events Observed	
		Yes	No
Events Forecast	Yes	A	B
	No	C	D

Table 2-1 2×2 contingency table with A referring to "hit" forecasts, B referring to "false alarm" forecasts, C referring to "missed" forecasts, and D referring to "correct rejections" or "correct negatives." N is often referred to as the sample size and equals A+B+C+D. The marginal totals for observations of the columns are calculated by A+C and B+D.

forecasts, "false alarm" forecasts, and "missed forecasts." After calculations, the best

threat score is 1 and the worse threat score is 0.

Chapter 3 Methodology

3.1 Event Selection

As a time saving measure, three cases from the ROCS archive were selected for further investigation. The cases are representative of a "hit," "false alarm," and "missed" forecast. The ROCS forecasts were issued from 2003 to 2008. The first thing that had to be done was to determine what seasons the forecasts should be taken from. It was decided that the best season to look at were the 2006 and 2007 season. The reason for this was that after 3 previous seasons of forecasting the ROCS group had increased the accuracy of their forecasts (further explained in chapter 5). The 2008 season was not chosen because the project was being wrapped up and forecasts were not made through the whole season.

The "hit" forecast that was chosen was issued between 1800 UTC on 30 November 2006 through 1800 UTC on 01 December 2006. The reason this forecast was chosen is that the forecasters were very certain on the occurrence of TSSN and it is a great representation of a "hit" forecast. The "false alarm" forecast was issued between 1800 UTC on 19 January 2007 through 1800 UTC on 20 January 2007. Finally the "missed" forecast was issued between 1800 UTC on 12 February 2007 through 1800 UTC on 13 February 2007. These forecasts were chosen because there were very few "false alarm" and "missed" forecasts made by the ROCS forecasters and these forecasts were the most representative.

3.2 Identification of Most Active Period

After the three cases have been decided upon, the most active period for each 24 hour forecast must be identified. To determine time, surface observations coded in METAR form are employed as well as data from the National Lightning Detection Network (NLDN). The METARs are scanned for the complete 24-hour period of the forecast looking for any mention of TSSN or snow with lightning distant. After TSSN has been identified by using the METAR data, they are checked again using the NLDN to confirm that there were actually lightning strikes. The METARs have to be corroborated with NLDN data because of inaccuracies in lightning detection by the Automated Surface Observing Systems (ASOS). It has been seen that the lightning detection instrumentation on the ASOS system doesn't necessarily catch lightning from TSSN events or the ASOS will record lightning when none actually occurred. This is less of a problem at major airports in the U.S. because they still employ human observers to back up the ASOS system.

After TSSN occurrence has been identified throughout the 24-hour forecast period a time is chosen right before most of the activity occurs. In the case of the "hit" event, 0000 UTC on 01 December 2006 was the time chosen to pull data for the event because most of the TSSN activity did not occur until after 0000 UTC. This same process was used for the "missed" event. It was determined that the time before the most activity was 0000 UTC on 13 February 2007. However, this process proves insufficient for the "false alarm" event because there is no TSSN activity associated with this event. In the case of the "false alarm" event, sleet with no lightning occurred instead of TSSN, so the time

chosen in relation to the height of the precipitation activity was 1200 UTC on 20

January, 2007. It is to be noted that only synoptic hours were chosen for these events.

3.3   Case Studies

There are many parts to the analysis process, so they have been broken up into

smaller sections to aid in the ease of describing the procedures. In section 3.2 a synoptic

hour for each event was decided upon and will be used to construct maps and other

analyses. To create our analyses, the Rapid Update Cycle (RUC) output was employed.

The RUC output employed were mapped to an 80-km grid and the grid spacing

corresponds to the model spacing that was used to create the forecasts. RUC output is

not real-time observation data, so this must be taken into account when analyzing the

maps. However, the RUC output is often the best representation of the atmosphere aloft

at times other than 0000 UTC and 1200 UTC. Archived data are compiled using the

GEMPAK Analysis and Rendering Program (GARP).

3.3.1   Outlook & Forecast Discussion

The original outlook maps and forecast discussions were created by the *ROCS*

group to inform the public on whether or not TSSN would develop and for where if

applicable. For this research the outlook maps and forecast discussion were not altered.

They appear just as they did when they were issued.

3.3.2   Analysis of Data from Original Forecast

To understand why the *ROCS* forecasters made the decision to issue a TSSN outlook or not issue a TSSN outlook, the data that they were using at the time must also be analyzed. This was gathered from the forecast discussions that were issued along with the outlook. In the forecast discussion the forecasters listed the model that they primarily used to back up their forecast and other information about model output as well as locations they were specifically focusing on. After this information was reviewed a sounding was made for each event from the original model data at the specific time and location they were focusing on.

3.3.3   Outcome

To determine the location and total snowfall from each event, snowfall maps were constructed by Doctor of Philosophy candidate Chad Gravelle from the Department of Earth and Atmospheric Sciences at St. Louis University for the specific use in this thesis.

3.3.4   Lightning Data

The lightning data for each case study comes from the NLDN which is accessed by using a data feed provided by Vaisala Inc. The lightning data from the NLDN are for the 48 contiguous United States and contain both in-cloud and cloud-to-ground lightning strikes.

3.3.5 Synoptic Analysis

For the synoptic analysis all of the mandatory levels are accessed, as well as moisture, vertical motion, and temperature. The mandatory levels are surface, 850-mb, 700-mb, 500-mb, and 300-mb. For the surface analysis METAR observations, geopotential thickness every 60 gpm, and mean sea level pressure at every 4 mb are plotted. The 850-mb and 700-mb analyses have upper-air observations, temperatures every 5°C, and geopotential heights every 30 gpm plotted. The 500-mb analysis has upper-air observations, geopotential heights every 60 gpm, and absolute vorticity every $4 \times 10^{-5} s^{-1}$ plotted. Finally the 300-mb analysis has upper–air observations, geopotential heights every 120 gpm, and isotachs every 20 kts plotted.

To measure the moisture content of the atmosphere for the events, maps are created with the mean relative humidity of 950-mb to 500-mb layer plotted. In order to determine if forcing for upward vertical motion is present during the events, Q-vectors are plotted to shows regions of vertical motion. The analysis for vertical motion has Q-vector divergence at every $-3 \times 10^{-16} \, m \, kg^{-1} \, s^{-1}$, Q-vectors, and potential temperature every $2 \, K$ plotted. Temperature is depicted in many of the maps that are created for the analysis, but one map was specifically created that uses thickness as a proxy for the actual temperature. A 5400 gpm thickness line often indicates the transition between snow and rain development (O'Hara et al., 2009). Although thickness analysis has been replaced by sounding analysis in recent years, it is still useful in determining rain/snow lines for a large spacial scale. The temperature map has thickness plotted from 1000-mb to 500-mb using geopotential meters.

3.3.6   Mesoscale & Sounding Analysis

The instability component in each of these events is a crucial part of this research so a few different methods are used to diagnose type and amount of instability in the atmosphere. The first map created for this purpose plots the lapse rate from 700- mb to 500-mb at every $-1\ K\ km^{-1}$. At this point soundings are created at times that start at the beginning of the activity throughout the duration of activity. The locations for the soundings in each event were chosen by their proximity to the greatest amount of lightning strikes. The exception to this approach involves the "false alarm" event. The sounding location that was chosen was at the center of the forecaster's outlook area. This way the location at the time of the initial forecast was expected to receive TSSN by forecasters.

Since TSSN cases may not result from upright convection, the next step is to create time-sections and cross-sections for the event. These provide a tool for diagnosing other possible types of instability. To create the cross-sections for each event the cross-section line was drawn perpendicular to the thickness gradient and if possible intersecting or in proximity to the sounding location for each event. For the cross-section analysis pseudo angular momentum at every $5\ kg\ m\ s^{-1}$, and equivalent potential temperature at every $2\ K$ were plotted. The time-sections were created at the same location the soundings were created. The time-section analysis has equivalent potential temperature plotted at every $2\ K$.

3.3.7 Remote Sensing Analysis

Two maps for each event were made using remote sensing data. The first map is a national composite of base radar reflectivity on a 1-km grid. The second map has infrared satellite imagery plotted with color enhancement.

3.3.8 Banding Identification Analysis

To confirm that mesoscale banding has occurred in a particular event base radar reflectivity must be used. Novak et al. (2003) developed classifications of mesoscale bands using base radar reflectivity (Table 3-1). The bands are identified using time and spatial scales. A single mesoscale band is present if it is greater than 250 km in length, it is between 20 and 100 km in width, and it has intensity greater than 30 dBZ for at least 2 hours. Multiple mesoscale bands are present if there are more than 3 bands with widths between 5 and 20 km, periodic spacing, same spatial orientation, and intensities greater than 10 dBZ of the background reflectivity for at least 2 hours. A narrow cold-frontal band is present if the band has a length greater than 300 km, a width between 10 and 50 km, it is located along a surface cold front or in the warm sector, and it occurs with intensities greater than 40 dBZ for at least 2 hours. A transitory band is present if the characteristics of the band meet the criteria of one of the other categories except for one. This usually applies to the lifetime of the band. An undefined band is a band that cannot be identified due to radar anomalies such as bright banding or missing data. The last classification is that of no banding present. This occurs if none of the criteria are meet for any if the other band categories. Using these classifications radar loops were created of

Band Type	Band Description
Single	Linear structure > 250 km in length, ~ 20–100 km in width, with an intensity > 30 dBZ maintained for at least 2 h
Multi	> 3 finescale (5–20 km width) bands with periodic spacing and of the same spatial orientation, with intensities > 10 dBZ over the background reflectivity, maintained for at least 2 h
Narrow Cold-frontal	Narrow (10–50 km), long (> 300 km) band found along surface cold front or in the warm sector with an intensity > 40 dBZ maintained for at least 2 h
Transitory	Structure that meets all respective criteria in a given category, except one (usually the lifetime)
Undefined	Ambiguous due to bright banding or incomplete radar data
Nonbanded	None of the above criteria are met

Table 3-1 Banding classifications from Novak et al. (2003).

the full 24 hour forecast periods and used to determine if banding occurred and what types of bands were occurring. Radar images are in 5 minute increments.

3.4 Verification Procedure

The verification part of this research uses all of the ROCS forecasts made between 2003 and 2007. The 2008 season was not included due to missing data. Every forecast was put into the category of being a "hit," false alarm," "missed," or a "correct rejection" forecast. The correct rejections will not be used in the verification analysis. Now that all the forecasts have been sorted into categories and tallied the threat score can be calculated using equation (5).

Chapter 4   Case Studies

4.1   01 December 2006 Case Study Analysis

4.1.1   Outlook & Forecast Discussion

For the "hit" case that occurred on 01 December 2006 the TSSN outlook was

created on 30 November 2006 at 1800 UTC and expired on 01 December 2006 at 1800

UTC. The outlook included a graphic that identified the location of any TSSN for the

next 24 hours. Figure 4.1 shows that TSSN was forecasted to occur in a swath from

extreme north Texas to Michigan. The outlook also included a forecast discussion

outlining the reasoning for the location and decision to issue a convective snow outlook.

Refer to Appendix A for the complete forecast discussion.

4.1.2   Analysis of Data from Original Forecast

To understand why the *ROCS* forecasters made their particular TSSN forecast

decision it is important to look at the data they were using. The model used primarily by

the forecasters for this event was the Global Forecast Model (GFS). In the forecast

discussion issued by *ROCS* it was mentioned that the necessary ingredients for TSSN

production would be in place over southern Missouri around 0600 UTC on 01 December

2006. Refer to Figure 4.2 for the location of the GFS model sounding. Joplin,
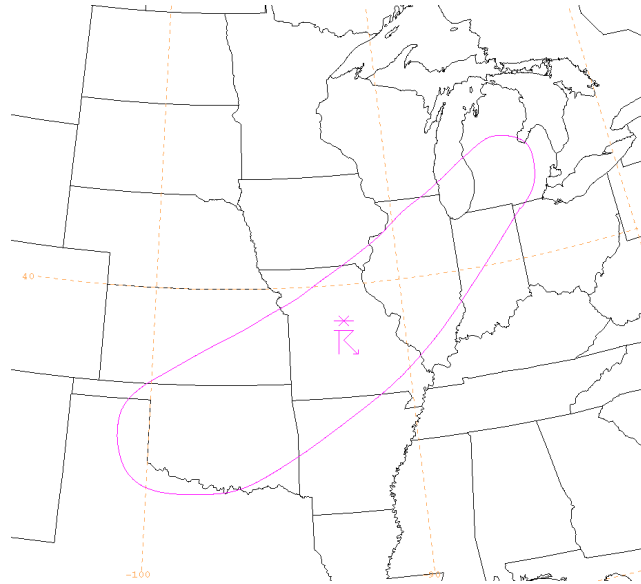
Figure 4.1 Indicates the location of forecasted TSSN from 1800 UTC on 30 November 2006 to 1800 UTC on 01 December 2006 (created by the *ROCS* group).

Figure 4.2 Outlook map for 1800 UTC on 30 November 2006 through 1800 UTC on 01 December 2006. Columbia, MO (sounding and time-section location) is identified on the map using a light blue star. The cross-section line from Des Moines, IA to Memphis, TN is identified on the map using a black line. Joplin, MO (GFS sounding location) is identified on the map using purple triangle.

MO, was chosen as a representative site for southern Missouri and is indentified with a purple triangle.

Figure 4.3 is the GFS 1200 UTC run with the 18-hr forecast sounding from Joplin, MO valid for 0600 UTC on 01 December 2006. 0600 UTC was choosen for the sounding time because in the original forcast disscusion the *ROCS* forecasters used the GFS 1200 UTC run with the 18-hour forecast. This would corespond to 0600 UTC on 01 December 2006. Using the same model run time and forecast time that the forecasters used enables understanding of why the forecasters made the decissions they did. The sounding depicts decent mean level moisture with relative humidity of 84%, and a profile that is unstable in the prefered lightning region of -10°C to -20°C (van den Broeke et al. 2005). The only problem with the sounding is that 700-mb to 500-mb lapse rates are weak. However, this problem was addressed by the forecasters in the forecast discussion and it was decided that with the present of elevated instability in the form of CAPE, a strong forcing mechanism to enable the release of that instabilty, and ample moisture would overcome the weak lapse rates and TSSN would be possible.

4.1.3 Outcome

Figure 4.4 depicts the actual snowfall amount (measured in inches) that was associated with the 01 December 2006 event. The location of the snowfall coincides with the outlook box issued by the forecasters at 1800 UTC on 30 November 2006. Western Missouri received the greatest snowfall totals from the event.
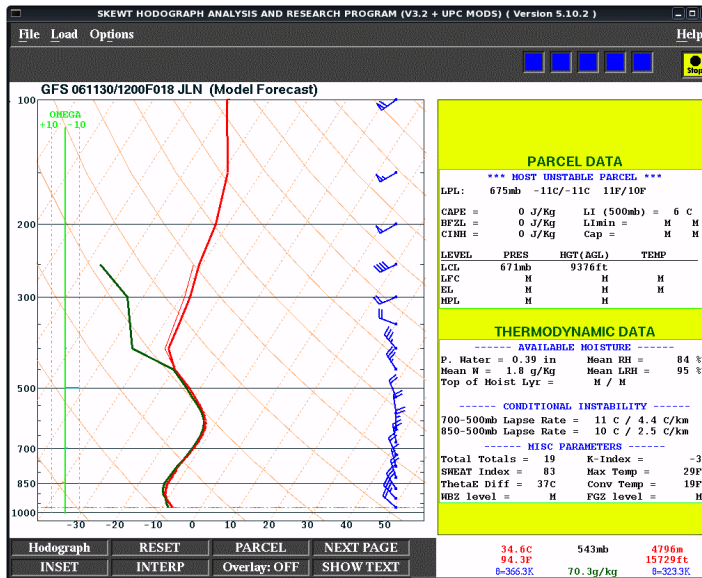
Figure 4.3 GFS 1200 UTC/18-hr forecast sounding for Joplin, MO (KJLN) valid on 01 December 2006 at 0600 UTC.

048h COOP SNOWFALL ending at 20061201 1200 UTC
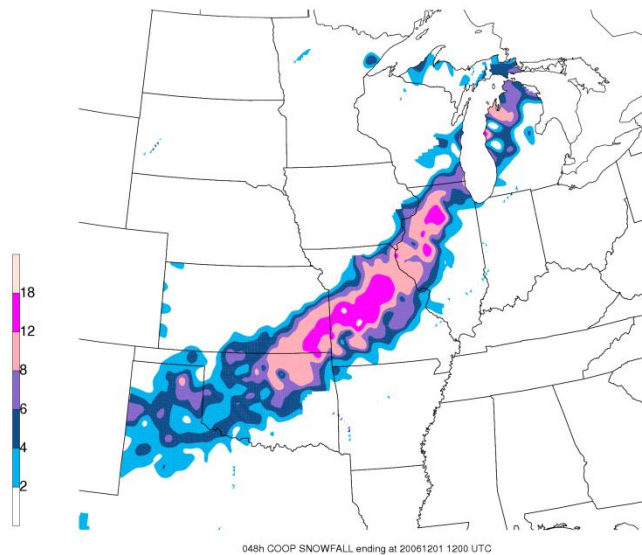
Figure 4.4 Total snowfall (every 2 in, filled contours starting at 2 in) map for 48 hours ending on 01 December 2006 at 1200 UTC (created by Chad Gravelle).

35

4.1.4 Lightning Data

Using data from the NLDN, a map has been constructed that depict the locations of in-cloud and cloud-to-ground lightning flashes associated with snowfall between 0600 UTC and 1200 UTC on 01 December 2006. This time period was chosen because there were ample lightning flashes during that period. Figure 4.5 depicts lightning flashes from the height of the event. All of the lightning flashes in the image have occurred within the outlook area.

4.1.5 Synoptic Analysis

All of the analyses for the synoptic analysis are based off of the 0000 UTC RUC initial fields for 01 December 2006. 0000 UTC on 01 December 2006 was chosen as the time for all the synoptic analyses because it bests depicts the system right before the greatest TSSN activity occurs. The surface analysis (Fig. 4.6) shows a surface low located to the southeast of Missouri. The surface low features two closed isobars suggesting that the cyclone has not yet reached the occlusion stage which typically requires a minimum of four closed isobars (Saucier 1955). The surface low is not extremely strong due to the fact that the lowest pressure for the system is above 1000-mb. Temperatures in southeastern Oklahoma, southern Missouri, northern Arkansas, and eastern Illinois are on the cusp between rain development and frozen precipitation development. The southern extent of the frozen precipitation in Figure 4.4 is located in those areas.

Figure 4.5 In-cloud (denoted by a dot) and cloud-to-ground (denoted by a negative or a positive sign) lightning flashes for 01 December 2006 between 0600 UTC and 1200 UTC. The graph on the bottom left side of the map displays the number of lightning flashes compared to the time they occurred. The time intervals are for every 60 minutes with the oldest lightning flashes being plotted on the far left of the graph and newest lightning flashes on the far right of the graph.

Figure 4.6 Surface analysis from the RUC initial fields with METAR observations in a standard station model configuration (black), geopotential thicknesses (every 60 gpm, dashed green lines) and mean sea level pressures (every 4 mb, solid blue lines) for 01 December 2006 at 0000 UTC.

37

The 850-mb analysis (Fig. 4.7) is useful in depicting the location of frontal zones. Through southeast Texas, Louisiana, and Arkansas thermal gradients are tighter than surrounding locations with colder air to the north and west of the tightened thermal gradient. This indicates cold air advection (CAA) and the location of the cold front. In through eastern Missouri, Illinois, Indiana, and Ohio there is also a tightened thermal gradient with warmer air located to the south and east of the tightened thermal gradient. This indicates warm air advection (WAA) and the location of the warm front.

The 700-mb analysis (Fig. 4.8) is similar to the 850-mb analysis but it can be particularly useful in identifying the mid-level components of the surface fronts and cyclone. In Figure 4.8 the upper level low pressure center is located upstream (eastern Oklahoma) from the surface low pressure center. CAA is present south and southwest of the mid-level cyclone in the regions of Texas, Louisiana, and Arkansas. WAA is present east and northeast of the mid-level cyclone in the regions of Missouri and Illinois. Smaller solenoids are often associated with stronger advection, so from this analysis it appears that the CAA is stronger than the WAA. Also, a weak trough of warm air aloft (TROWAL) signature may be present in the regions of Missouri and Kansas.
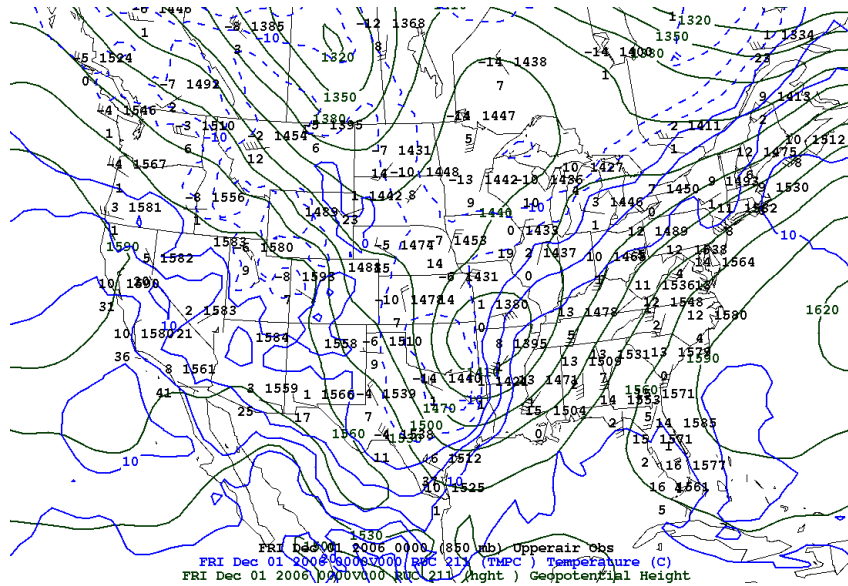
Figure 4.7 Analysis from the RUC initial fields for 850-mb with upper-air station models (black), temperatures (every 5 Cº, solid and dashed blue lines) and geopotential heights (every 30 gpm, solid green lines) for 01 December 2006 at 0000 UTC.
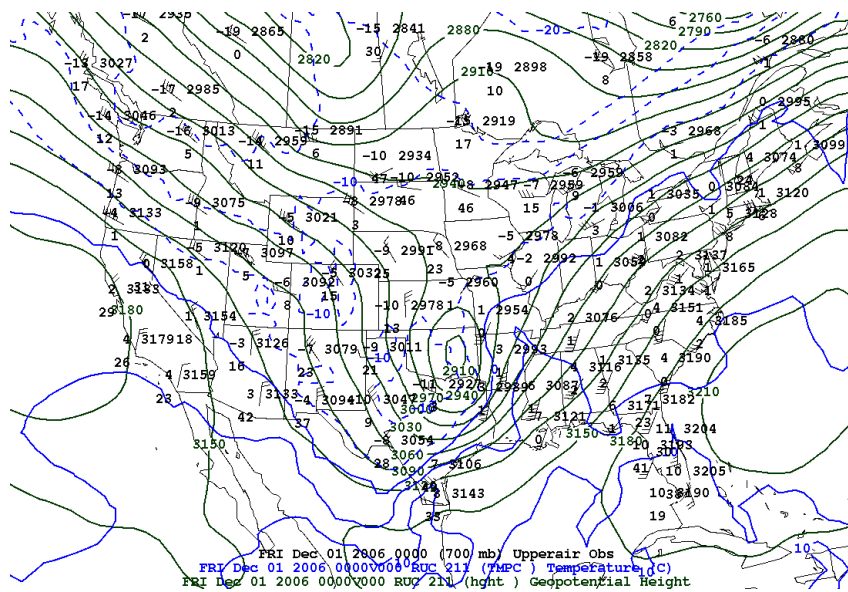
Figure 4.8 Analysis from the RUC initial fields for 700-mb with upper-air station models (black), temperatures (every 5 Cº, solid and dashed blue lines) and geopotential heights (every 30 gpm, solid green lines) for 01 December 2006 at 0000 UTC.

The 500-mb analysis (Fig. 4.9) is useful in determining the amount of vorticity and vorticity advection in the current atmosphere. When using the assumptions of quasi-geostrophic (Q-G) theory, cyclonic vorticity advection (CVA) can be associated with upward vertical motion. In Figure 4.9 there is strong cyclonic vorticity advection (CVA) located in northern Texas and Oklahoma, indicating convergence at the surface and divergence aloft. The vorticity maximum is located in northeastern Texas and southeastern Oklahoma.

The 300-mb analysis (Fig. 4.10) is useful in determining the location of the upper level jet streams and subsequent jet streaks. In Figure 4.10 there is a jet streak located in eastern Texas extending into western Arkansas with winds speeds of 140 kts. A smaller jet streak is located in the region near Wisconsin with wind speeds of 140 kts. With the location of the jet streak in Texas and western Arkansas, upward vertical motion would be expected in southern Texas, eastern Oklahoma, eastern Kansas, and western Missouri. With the other jet streak being located near Wisconsin, upward vertical motion would be expected in northern Illinois and western Arkansas.
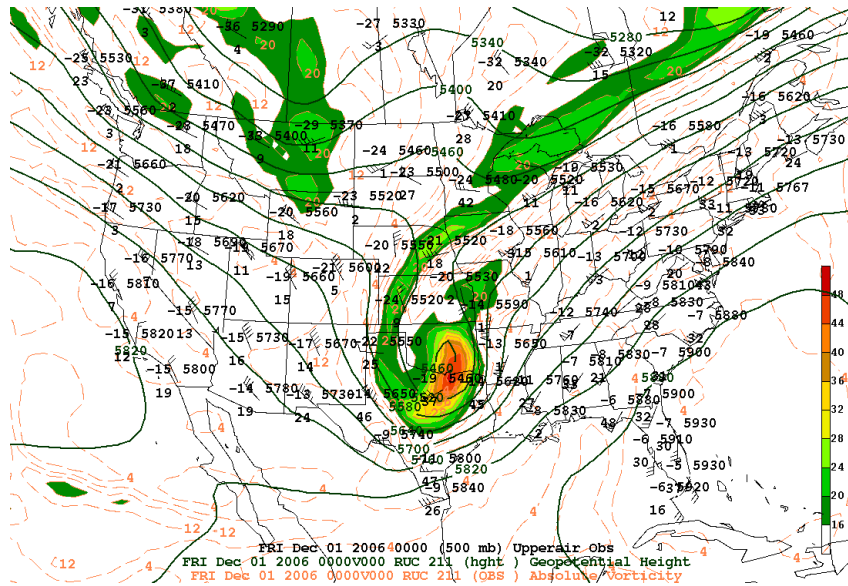
Figure 4.9 Analysis from the RUC initial fields for 500-mb with upper-air station models (black), geopotential heights (every 60 gpm, solid green lines), and absolute vorticity ($1 \times 10^{-5}\ s^{-1}$ with an interval of $4 \times 10^{-5}\ s^{-1}$, solid with filled contours that begin at $16 \times 10^{-5}\ s^{-1}$) for 01 December 2006 at 0000 UTC.
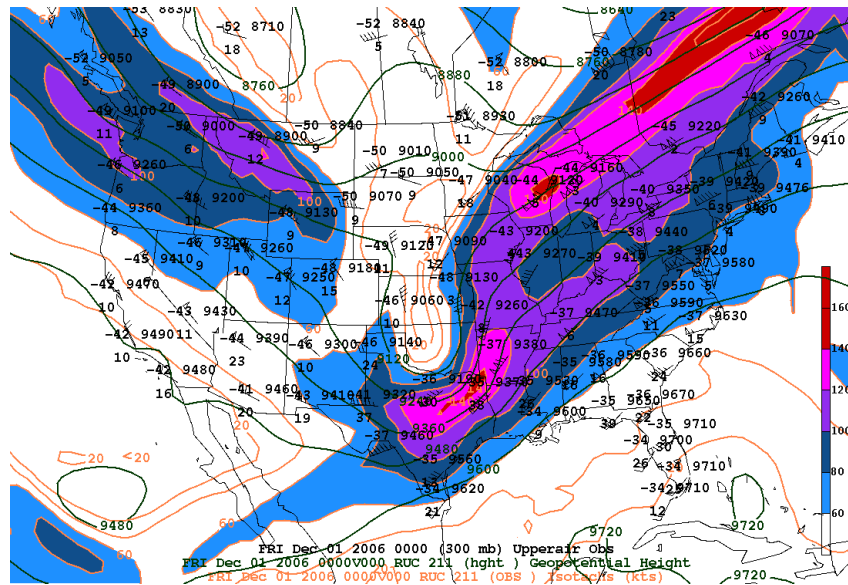
Figure 4.10 Analysis from the RUC initial fields for 300-mb with upper-air station models (black), geopotential heights (every 120 gpm, solid green lines), and isotachs (every 20 kts, shaded contours over 60 kts) for 01 December 2006 at 0000 UTC.

Figure 4.11 depicts low-level relative humidity from 950-mb to 500-mb. Much of the original outlook area that includes northwestern Texas, Oklahoma, Missouri, Illinois, Indiana, and Michigan contain relative humidities greater than 80% indicating sufficient moisture for convection, cloud development, and precipitation processes.

Figure 4.12 depicts Q-vector divergence with filled contours. From this map upward vertical motion is occurring in eastern Oklahoma, Kansas, much of Arkansas, western Missouri, and in other parts of the outlook area.

Geopotential thickness is useful in determining what type of precipitation is possible for a specific region because it helps a forecaster to determine the average temperature within a layer. Typically the 540 decameter (dam) thickness line is the rain/snow line with lower thickness numbers associated with cold air and higher thickness numbers associated with warmer air. From this analysis (Fig. 4.13) the outlook area appears to be cold enough for snow production.
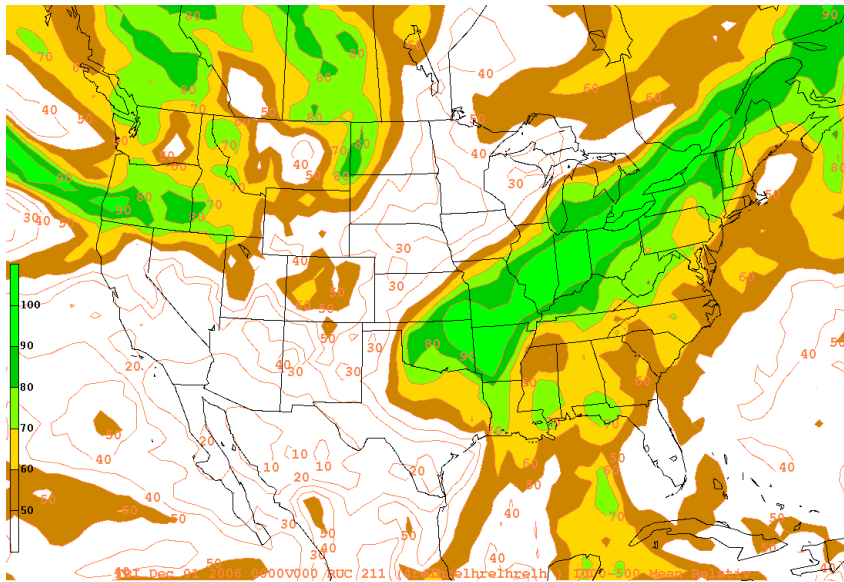
Figure 4.11 Relative humidity from the RUC initial fields (%, solid with filled contours that begin at 50%) from 950-mb to 500-mb for 01 December 2006 at 0000 UTC.
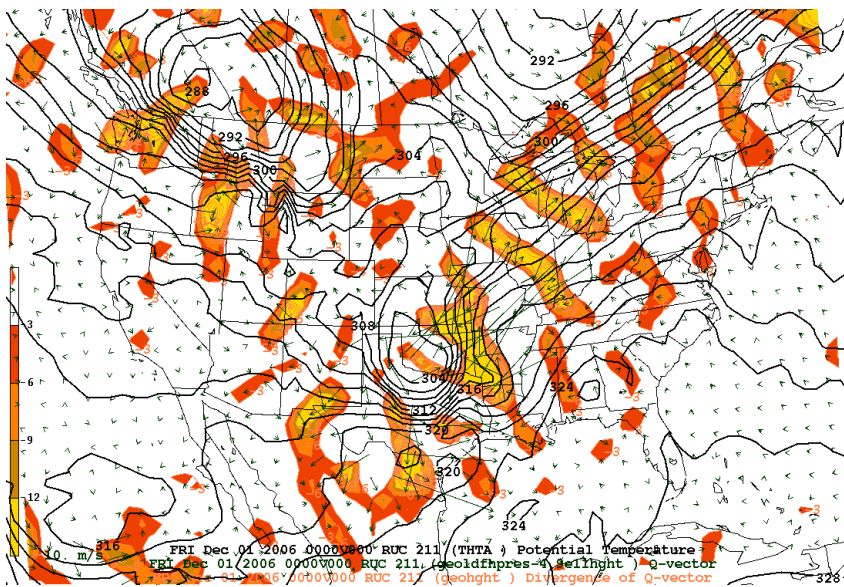
Figure 4.12 700-mb to 300-mb Q-vector divergence from the RUC initial fields ($m\ kg^{-1}\ s^{-1}$ with an interval of $-3 \times 10^{-16}\ m\ kg^{-1}\ s^{-1}$ solid and filled), 700-mb to 300-mb Q-vectors from the RUC initial fields (green arrows) and 500-mb potential temperature from the RUC initial fields (every 2 K, solid black lines) for 01 December 2006 at 0000 UTC.
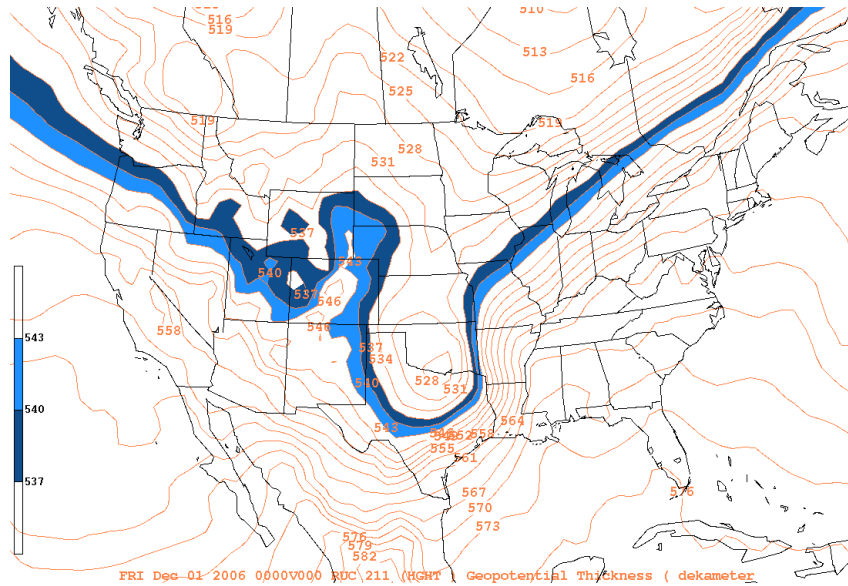
Figure 4.13 Geopotential thickness from the RUC initial fields for 1000-mb to 500-mb (every 3 dam, solid with filled contours starting at 537 dam) for 01 December 2006 at 0000 UTC.

4.1.6 Mesoscale & Sounding Analysis

The instability analysis is extremely important because it determines if the atmosphere possesses enough instability for convection to occur if that instability is released. From previous research performed by the *ROCS* group, it was determined that the best lapse rates using the 700-mb to 500-mb layer for the development of TSSN is $-6.5\ K\ km^{-1}$ or less. In the outlook region the lapse rates are not $-6.5\ K\ km^{-1}$ or less but TSSN still developed in the outlook region (Fig. 4.14).

Skew-T soundings are extremely useful in determining instability, moisture, and temperature profiles of the atmosphere. 0400 UTC, 0600 UTC, and 0800 UTC on 01 December 2006 were chosen for the sounding analyses because these times correspond to the greatest TSSN activity of the event. 0600 UTC on 01 December 2006 is the best sounding time for the event in respect to TSSN activity and is used in the cross-section

44

analysis. Columbia, MO was chosen for the location of the soundings, and the time-section because a large amount of lightning flashes occurred in the area.

Figure 4.15 is the 0400 UTC RUC model sounding for Columbia, MO. Refer to Figure 4.2 for the outlook map with the sounding location identified by a blue star. The sounding reveals a mean relative humidity of 95%, a 700-mb to 500-mb lapse rate of $-4.8\ K\ km^{-1}$, an almost saturated atmosphere throughout most of the troposphere, and temperatures at or below 0°C. In the preferred lightning region between -10°C and -20°C (van den Broeke et al. 2005), the sounding approaches moist neutral. Analysis of this sounding reveals that TSSN development is likely in the sounding region.

Figure 4.16 is the 0600 UTC sounding. The difference between the 0600 UTC and the 0400 UTC sounding is that the mean relative humidity drops to 91%, and the lapse rate is $-5.3\ K\ km^{-1}$ which in this case indicates slightly greater instability. The 0600 UTC sounding is more conducive to TSSN.

Figure 4.17 is the 0800 UTC sounding. This sounding shows that the event is starting to wrap up. The relative humidity has dropped to 89% and the lapse rate has become less negative indicating a decrease in instability. The likelihood of TSSN is starting to decrease for the area at this time.

45
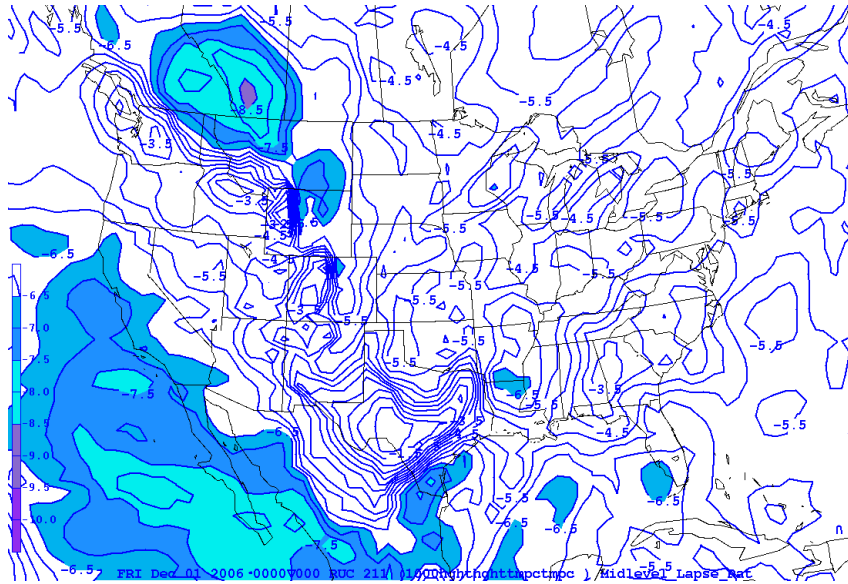
Figure 4.14 **Lapse rates from the RUC initial fields for 700-mb to 500-mb (every − 1 $K\ km^{-1}$, solid with filled contours starting at − 6.5 $K\ km^{-1}$) for 01 December 2006 at 0000 UTC.**
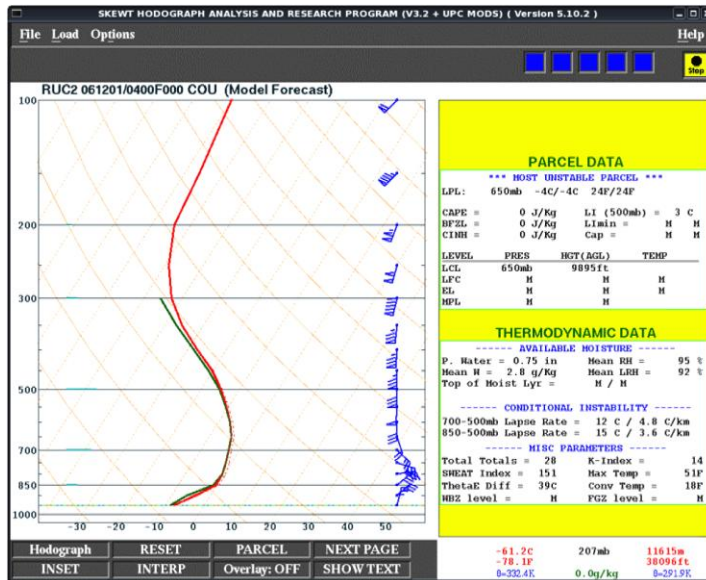
Figure 4.15 **Sounding from the RUC initial fields for Columbia, MO (KCOU) valid on 01 December 2006 at 0400 UTC.**
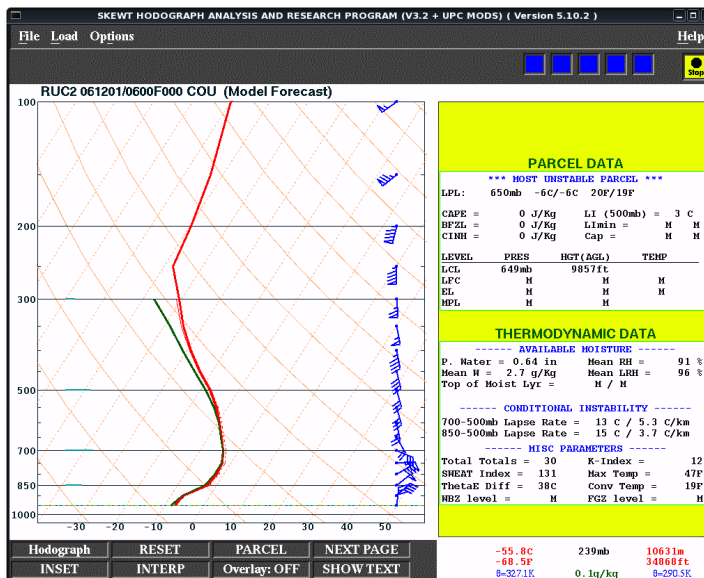
Figure 4.16 Sounding from the RUC initial fields for Columbia, MO (KCOU) valid on 01 December 2006 at 0600 UTC.
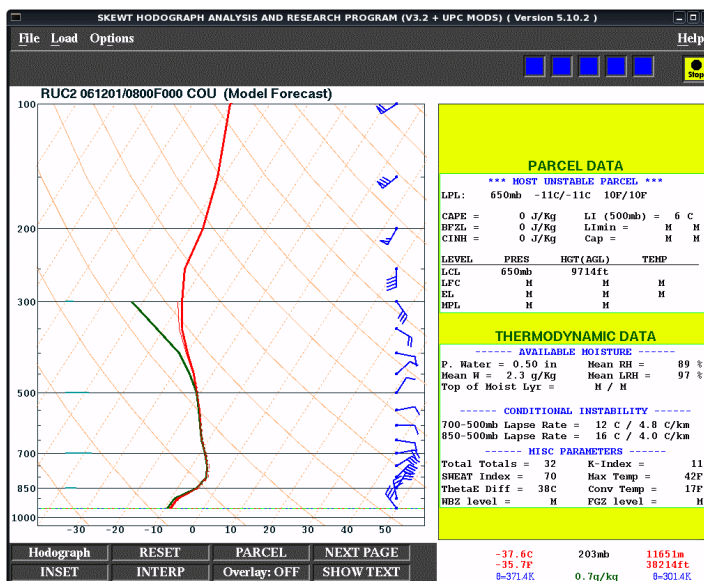
Figure 4.17 Sounding from the RUC initial fields for Columbia, MO (KCOU) valid on 01 December 2006 at 0800 UTC.

Besides sounding and lapse rate analysis, isentropic analysis can be useful for accessing the instability of a system. For this analysis, potential temperature (θ_e), pseudo-angular momentum (M_g), and relative humidity from 1000-mb to 300-mb is plotted. Refer to Figure 4.2 for the outlook map with the cross-section line drawn in black from Des Moines, IA to Memphis, TN. This cross-section line was chosen because it is drawn parallel to the thickness gradient and almost intersects the sounding location of Columbia, MO. Figure 4.18 is the actual cross-section. Throughout eastern Kansas and southwest Missouri the potential temperature lines between 700-mb and 300-mb are becoming further apart from each other, indicating increased instability in that layer. Also, with the slope of the M_g being much greater that of the slope of θ_e conditional instability may be present since the atmosphere is saturated with respect to ice.

Figure 4.19 is the time-section from 1800 UTC on 30 November 2006 through 1800 UTC on 01 December 2006 for Columbia, MO. Refer to Figure 4.2 for the outlook map with the time-section location identified by a light blue star. The time-section depicts equivalent potential temperature surfaces increasing in slope troughout much of the 700-mb to 500-mb layer between 0600 and 0900 UTC indicating that the atmosphere is moist neutral in that area for that particular time series.

48
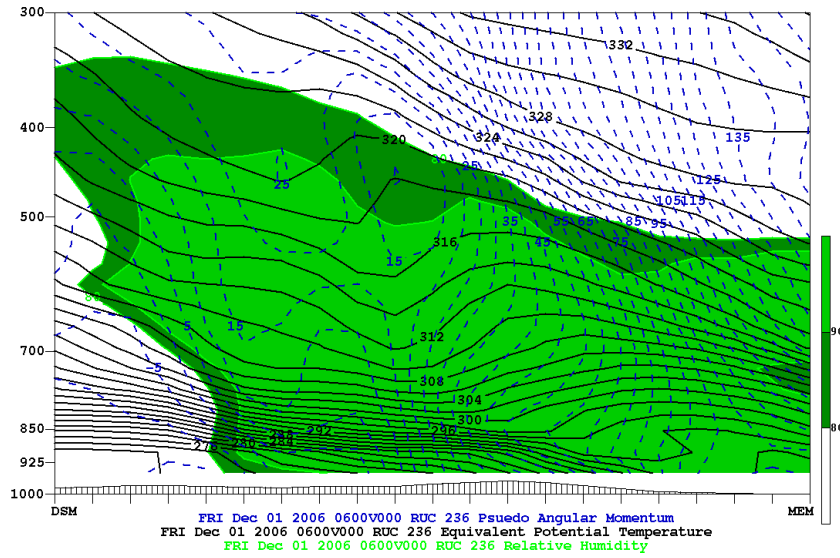
Figure 4.18 **1000-mb to 300-mb space cross-section from the RUC initial fields with psuedo-angular momentum (every 5 $kg\ m\ s^{-1}$, dashed blue lines), equivalent potential temperatures (every 2 K, solid black lines), and relative humidity (%, solid with filled contours that begin at 80%) from Des Moines, IA to Memphis, TN valid on 01 December 2006 at 0600 UTC.**
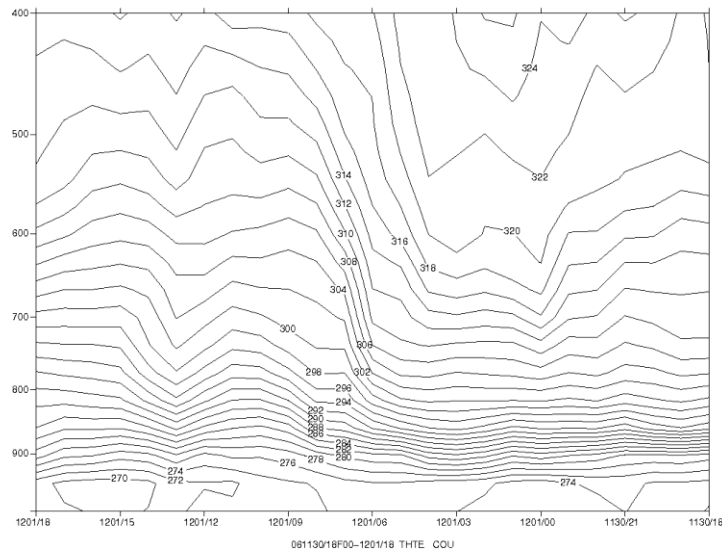
Figure 4.19 **1000-mb to 400-mb time-section from the RUC initial fields with equivalent potential temperatures (every 2 K, solid black lines) from 1800 UTC on 30 November 2006 through 1800 UTC on 01 December 2006 for Columbia, MO. Time increases on the abscissa from right to left.**

49

4.1.7 Remote Sensing Analysis

The radar and satellite data analyses offer a glimpse of the intensity of the system as well as location of the precipitation and cloud cover. 2359 UTC and 2345 UTC on 30 November 2006 was chosen for the radar and satellite analyses because they are the closest possible data times to 0000 UTC on 01 December 2006. The times for the radar and satellite analyses need to be close to 0000 UTC on 01 December 2006 to match with the synoptic analyses.

Figure 4.20 depicts base radar reflectivity for 2359 UTC on 30 November 2006. There is widespread radar reflectivity throughout most of the outlook area and 30 to 35 dBZ reflectivity through southern Missouri, and western Illinois. There is also a small area of 50+ dBZ in eastern Indiana. This reflectivity indicates widespread precipitation is associated with this system.

Figure 4.21 depicts infrared satellite data from 2345 UTC on 30 November 2006. The image displays widespread cloud coverage through much of the outlook area with cloud top temperatures of -60°C or less in southeastern Missouri and central to north central Illinois.

4.1.8 Banding Identification Analysis

Crowe et al. (2006) have shown that even though the heavy snowfall is not always associated with TSSN, if TSSN does occur with a system then it is likely that heavy snowfall will occur at some point and location in the system's lifecycle. Using Novak et al.'s (2003) criteria for determining precipitation bands using radar reflectivity, Figure 4.22 shows the location of a long-lived single snow band that set up in eastern Missouri
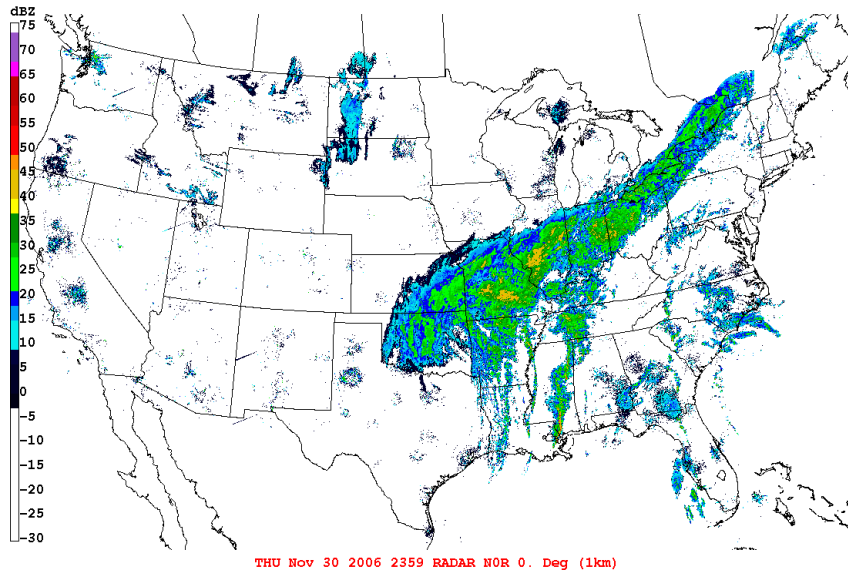
Figure 4.20 Base radar reflectivity for 30 November 2006 at 2359 UTC. The legend on left is a color table, binned every 5 dBZ.
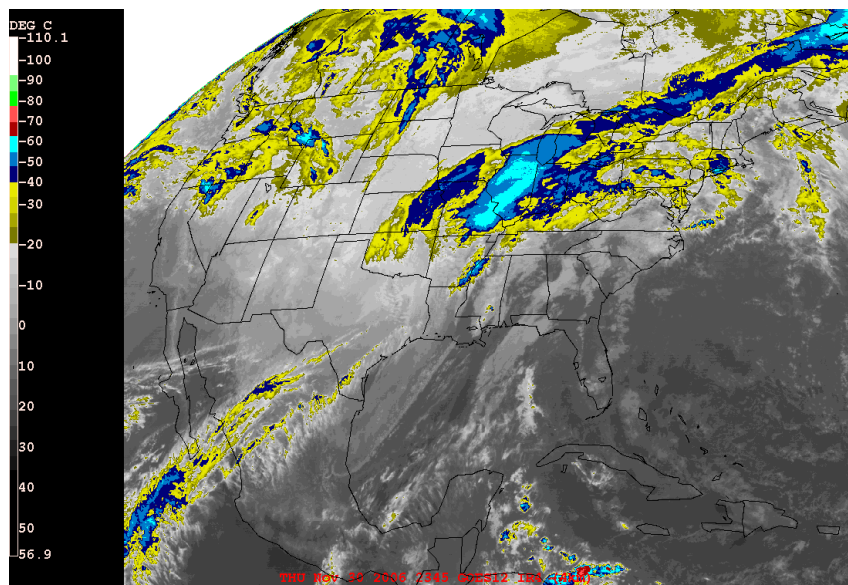
Figure 4.21 Infrared satellite imagery with color enhancement for 30 November 2006 at 2345 UTC. The legend on the left is a color table, binned every 10°C.

51
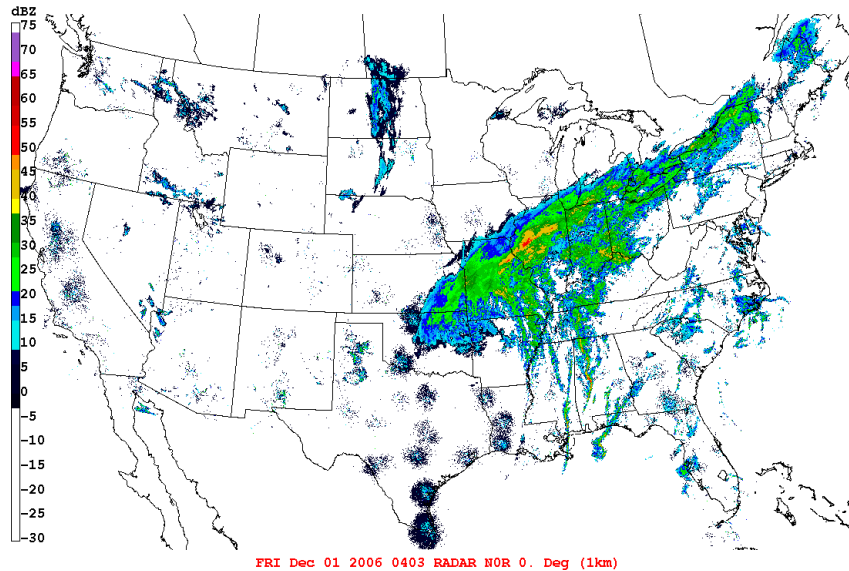
Figure 4.22 Base radar reflectivity for 01 December 2006 at 0403 UTC. The legend on left is a color table, binned every 5 dBZ.

and central Illinois. This band correlates positively with the heaviest snowfall totals in

Figure 4.2.

4.1.9   Summary

The 01 December 2006 "hit" forecast event proved relatively easy for the

forecasters to predict. Temperatures were cold enough for snow development, there was

sufficient moisture associated with the system for deep, moist convection, there was

significant forcing for accent, and the thermal profiles approached moist neutral in the

soundings from the RUC initial fields. Model solutions from the GFS were adequate and

interpreted properly by the *ROCS* forecasters.

4.2   20 January 2007 Case Study Analysis

4.2.1   Outlook & Forecast Discussion

For the "false alarm" event that occurred on 20 January 2007, a TSSN outlook was created for the period from 1800 UTC on 19 January 2007 to 1800 UTC on 20 January 2007. The outlook included a graphic that identified the location of any TSSN for the next 24-hours. Figure 4.23 shows that TSSN was forecasted to occur in swath from Oklahoma, through central and western Kansas, Missouri, southern Iowa, and into west central Illinois. The outlook also included a forecast discussion outlining the reasoning for the location and decision to issue a convective snow outlook. The complete forecast discussion is shown in Appendix B.

4.2.2   Analysis of Data from Original Forecast

To understand why the *ROCS* forecasters made their particular TSSN forecast decision it is important to look at the data they were using. The model used primarily by the forecasters for this event was the Global Forecast Model (GFS). In the forecast discussion issued by *ROCS*, convective snow was anticipated for the outlook region because model guidance suggested colder temperatures (0°C to -10°C) throughout the lower troposphere in northern Texas and southern Oklahoma, ample moisture in the outlook area, and strong forcing for accent. It was mentioned by the forecasters that with lapse rates greater than $-5.8\ K\ km^{-1}$, the system may not be unstable enough for
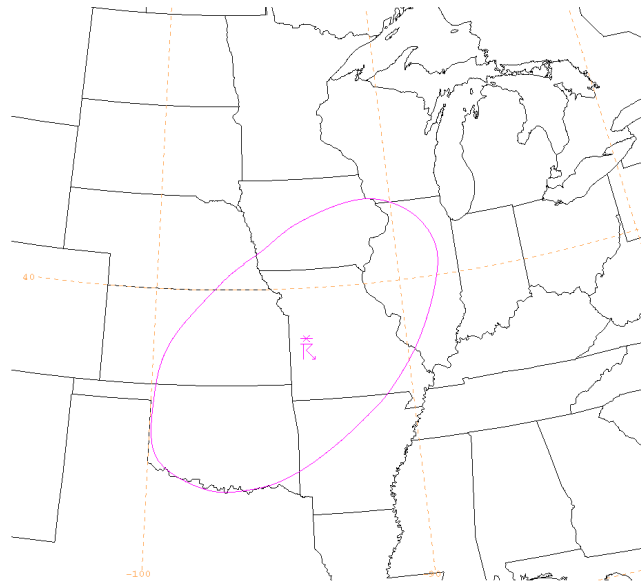
Figure 4.23 Indicates the location of forecasted TSSN from 1800 UTC on 19 January 2007 to 1800 UTC on 20 January 2007 (created by the *ROCS* group).

lightning production, but they assumed with cold enough temperatures, some lightning

could develop. Refer to Figure 4.24 for the location of the GFS model sounding. Figure

4.25 is the GFS 1200 UTC 30-hr forecast sounding for Canadian, TX (KHHF) valid at

1800 UTC on 20 January 2007. This sounding location was chosen because the *ROCS*

forecasters mentioned it in their forecast discussion and 1800 UTC on 20 January 2007

was used for the forecasting time because the forecasters predicted snowfall to occur in

the forecast outlook area by that time. Figure 4.25 shows the weaker lapse-rates and

colder temperatures predicted by the model.
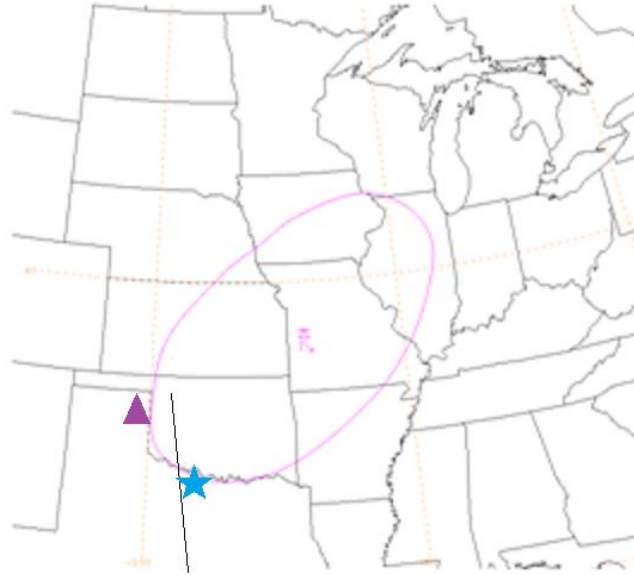
Figure 4.24 Outlook map for 1800 UTC on 19 January 2007 through 1800 UTC on 20 January 2007. Wichita Falls, TX (sounding and time-section location) is indentified on the map using a light blue star. The cross-section line from Woodward, OK to Austin, TX is identified on the map using a black line. Canadian, TX (GFS sounding location) is identified on the map using purple triangle.
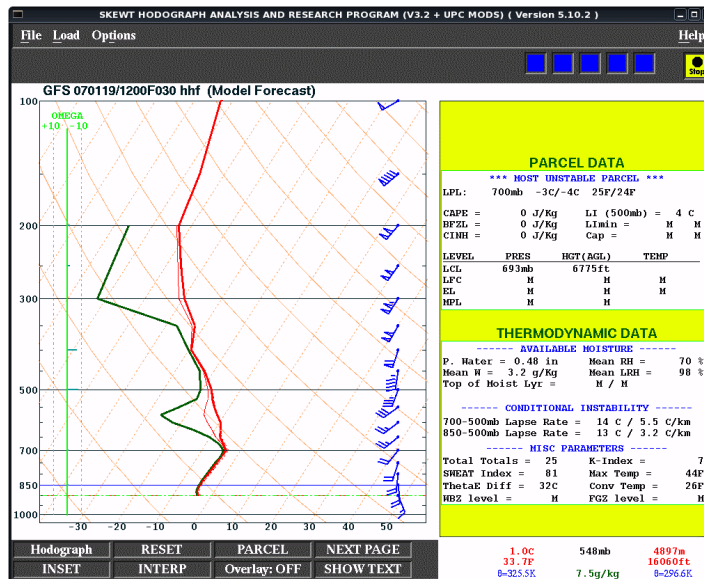
Figure 4.25 GFS 1200 UTC/30-hr forecast sounding for Canadian, TX (KHHF) valid on 20 January 2007 at 1800 UTC.

55

4.2.3 Outcome

Figure 4.26 depicts the actual snowfall amount (measured in inches) that was associated with the 20 January 2007 event. The location of the snowfall coincides with a large amount of the outlook graphic issued by the forecasters at 1800 UTC on 19 January 2007. Northwestern Texas, western Kansas, and central Nebraska received the greatest snowfall totals from the event.

4.2.4 Lightning Data

Using data from the NLDN, it was determined that there were no in-cloud or cloud-to-ground lightning flashes associated with snowfall in the period between 19 January 2007 at 1800 UTC and 20 January 2007 at 1800 UTC for the outlook region. With no lightning associated with this event it can only be classified as a "false alarm."

072h COOP SNOWFALL ending at 20070122 1200 UTC
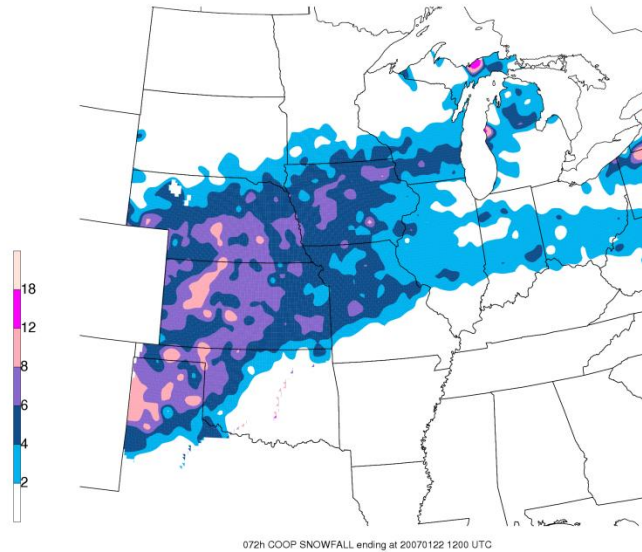
Figure 4.26 Total snowfall (every 2 in, filled contours starting at 2 in) map for 72 hours ending at 22 January 2007 on 1200 UTC (created by Chad Gravelle).

4.2.5   Synoptic Analysis

All of the analyses for the synoptic levels are based off of the 1200 UTC RUC

initial fields for 20 January 2007. 1200 UTC on 20 January 2007 was chosen as the time

for the synoptic analyses because this time bests depicts the system right before the TSSN

activity was expected to occur. The surface analysis (Fig. 4.27) shows a poorly defined

low pressure center located in northern Arizona and New Mexico with the lowest

pressure in that area greater than 1000-mb. The system appears very weak and

unorganized. Temperatures are cold enough at the surface for frozen precipitation in

large portions of Kansas, Missouri, Iowa, and Illinois.

57
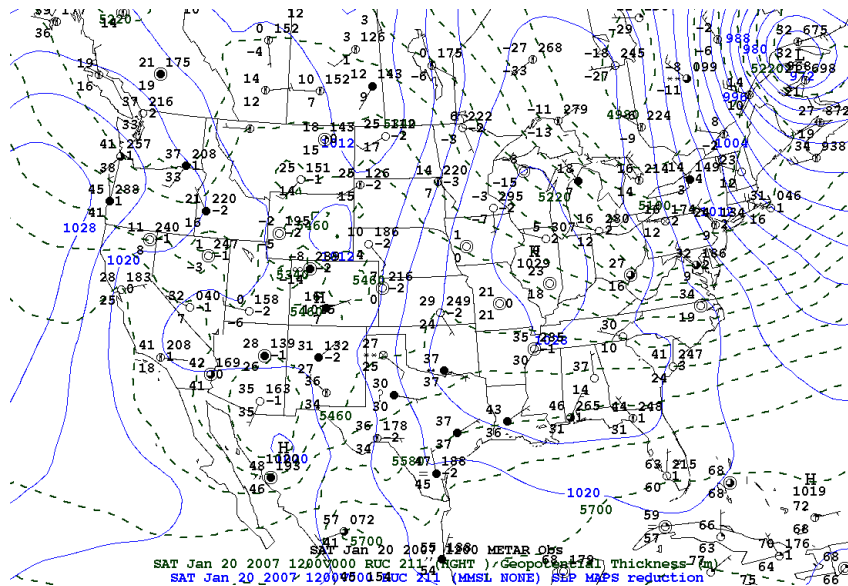
Figure 4.27 Surface analysis from the RUC initial fields with METAR observations in a standard station model configuration (black), geopotential thicknesses (every 60 gpm, dashed green lines) and mean sea level pressures (every 4-mb, solid blue lines) for 20 January 2007 at 1200 UTC.

The 850-mb analysis (Fig. 4.28) is not clear enough to accurately pinpoint the location of the warm and cold fronts associated with the system. WAA and CAA appear to be very weak at this level due to the fact that there are very few solenoids, let alone small solenoids to indicate strong WAA or CAA. The 700-mb analysis (Fig. 4.29) more clearly depicts the low pressure center of the system located mostly in Arizona than the surface and 850-mb analyses. WAA and CAA still appear to be weak with this system. The 500-mb analysis (Fig. 4.30) depicts some CVA in northern western Mexico, western Arizona, and eastern New Mexico, but CVA is significantly weaker in this event then with the "hit" event. Weaker CVA can also indicate weaker upward vertical motions, with less convergence at the surface and less divergence aloft.   The vorticity maximum is located in northwestern Mexico.
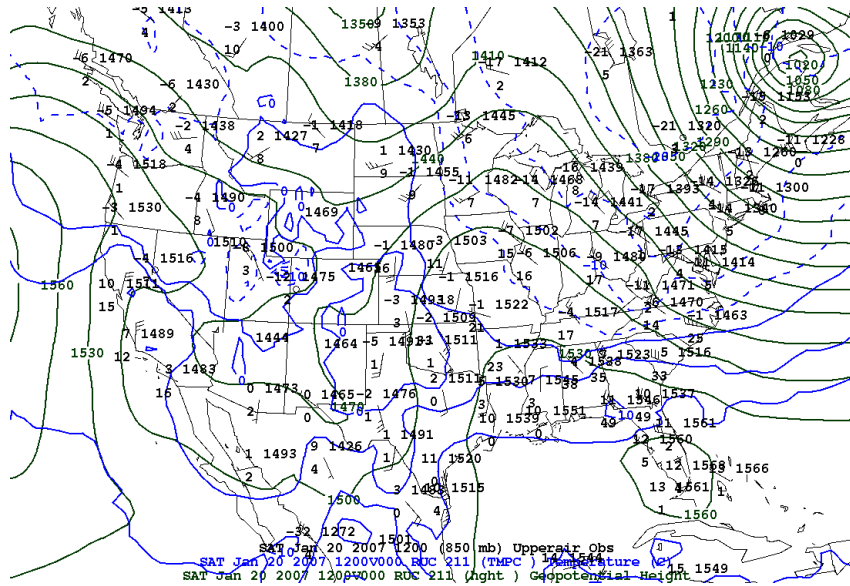
Figure 4.28 Analysis from the RUC initial fields for 850-mb with upper-air station models (black), temperatures (every 5 Cº, solid and dashed blue lines) and geopotential heights (every 30 gpm, solid green lines) for 20 January 2007 at 1200 UTC.
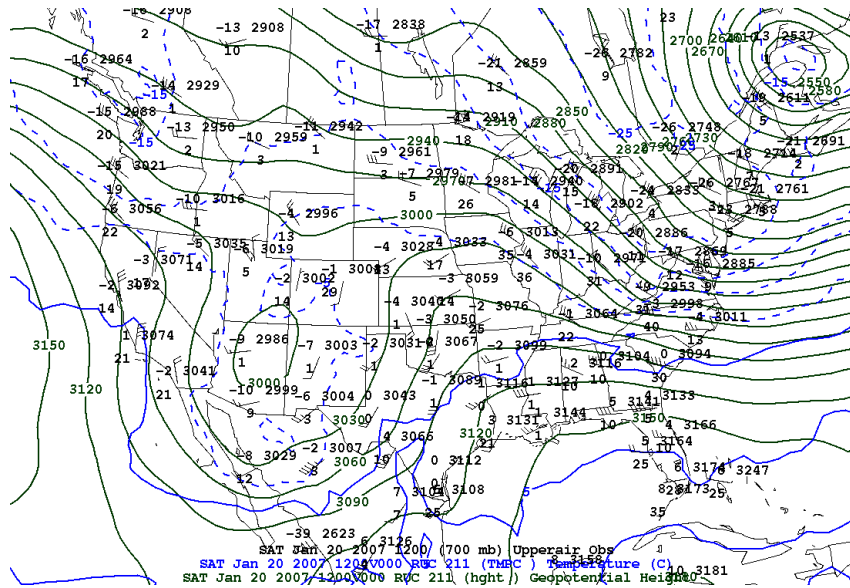
Figure 4.29 Analysis from the RUC initial fields for 700-mb with upper-air station models (black), temperatures (every 5 Cº, solid and dashed blue lines) and geopotential heights (every 30 gpm, solid green lines) for 20 January 2007 at 1200 UTC.
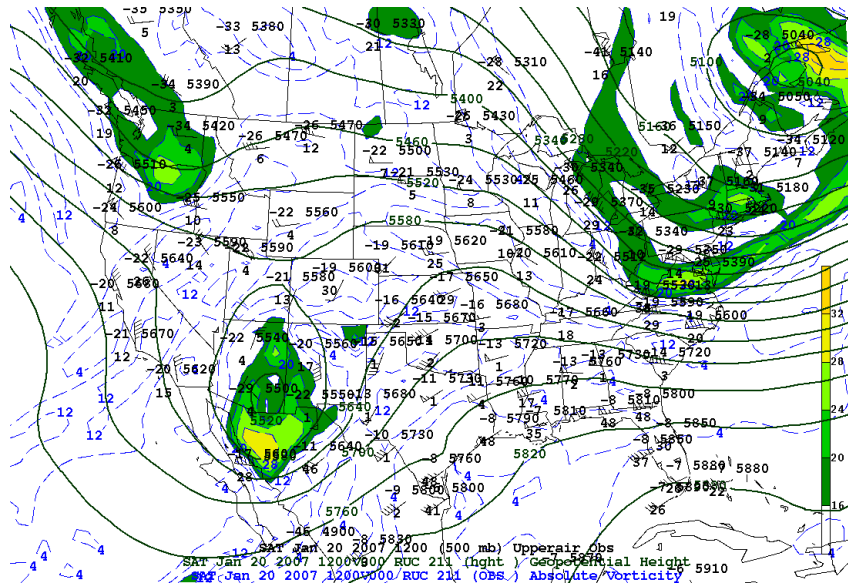
Figure 4.30 Analysis from the RUC initial fields for 500-mb with upper-air station models (black), geopotential heights (every 60 gpm, solid green lines), and absolute vorticity ($1 \times 10^{-5}\ s^{-1}$ with an interval of $4 \times 10^{-5}\ s^{-1}$, solid with filled contours that begin at $16 \times 10^{-5}\ s^{-1}$) for 20 January 2007 at 1200 UTC.

The 300 mb analysis (Fig. 4.31) shows a jet steak located in northwestern Mexico moving into New Mexico and Texas with wind speeds of 120 kts. The location of the jet streak indicates that upward vertical motion may be enhanced in the regions of New Mexico, and northwestern Texas.

Figure 4.32 depicts low level relative humidity from 950-mb to 500-mb. Some of the outlook area appears to be relatively dry but parts of Oklahoma and Kansas have relative humidities greater than 80% and as the system moves northeastward moisture will begin to advect into the drier areas.

Figure 4.33 depicts Q-vector divergence with filled contours. From Figure 4.33, locations of upward vertical motion are New Mexico, western Texas, central Oklahoma, as well as parts of Kansas, Missouri, and Iowa.

60
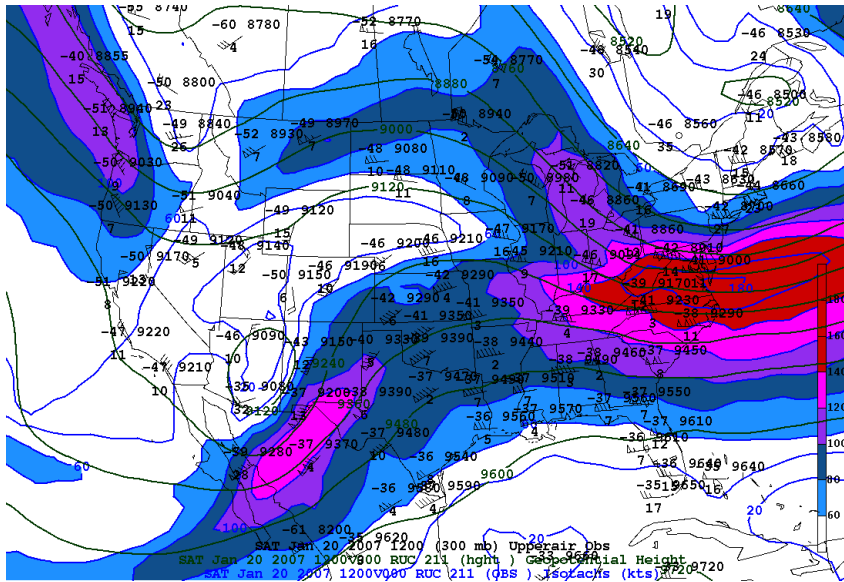
Figure 4.31 Analysis from the RUC initial fields for 300-mb with upper-air station models (black), geopotential heights (every 120 gpm, solid green lines), and isotachs (every 20 kts, shaded contours over 60 kts) for 20 January 2007 at 1200 UTC.
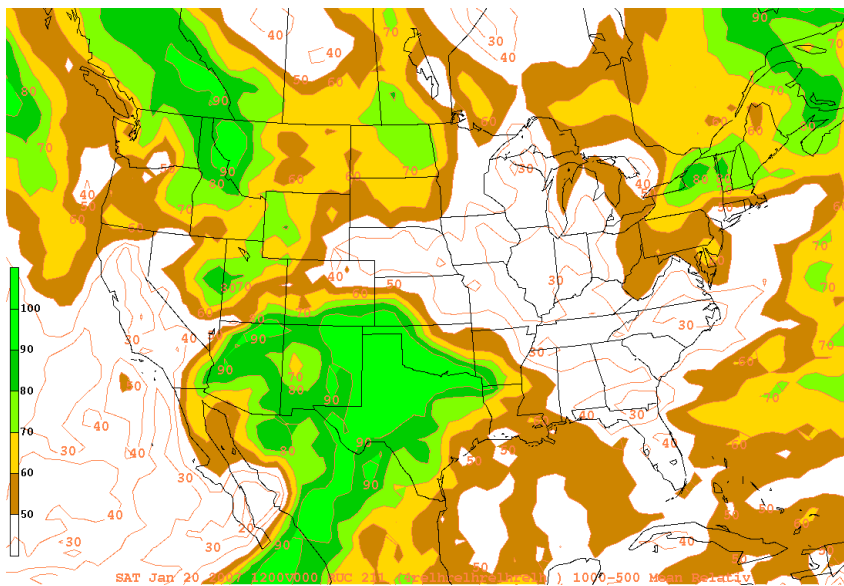
Figure 4.32 Relative humidity from the RUC initial fields (%, solid with filled contours that begin at 50%) for 950-mb to 500-mb for 20 January 2007 at 1200 UTC.

61
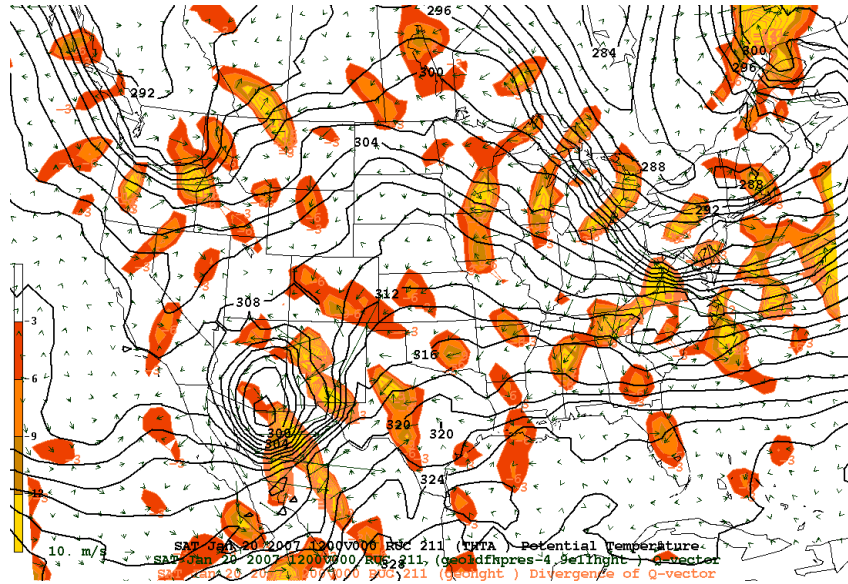
Figure 4.33 **700-mb to 300-mb Q-vector divergence from the RUC initial fields ($m\ kg^{-1}\ s^{-1}$ with an interval of $-3 \times 10^{-16}\ m\ kg^{-1}\ s^{-1}$ solid and filled), 700-mb to 300-mb Q-vectors from the RUC initial fields (green arrows) and 500-mb potential temperature from the RUC initial fields (every 2 K, solid black lines) for 20 January 2007 at 1200 UTC.**

Based on thickness analysis (Figure 4.34), it appears that most of the outlook area is in a region with thicknesses greater than 540 dam. This may indicate that the outlook region may be too warm for snow production.
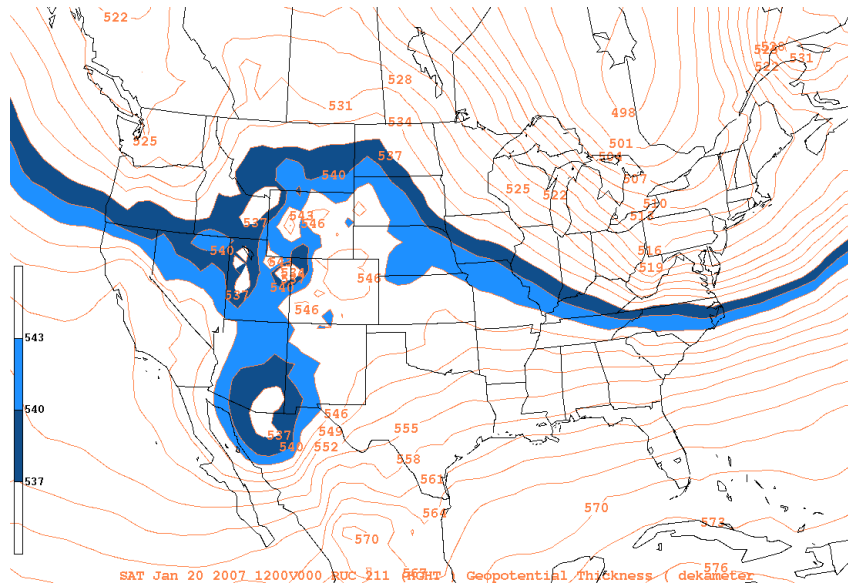
Figure 4.34 Geopotential thickness from the RUC initial fields for 1000-mb to 500-mb (every 3 dam, solid with filled contours starting at 537 dam) for 20 January 2007 at 1200 UTC.

4.2.6   Mesoscale & Sounding Analysis

In Figure 4.35 lapse rates are contoured and filled anywhere the lapse rate is $-6.5 \, K \, km^{-1}$ or less. In western Arizona and southwestern New Mexico lapse rates are $-7 \, K \, km^{-1}$ or less indicating an unstable environment for those areas and as the system moves northeastward lapse rates in the outlook region should become more unstable. The more unstable the outlook region becomes, the more likely TSSN will occur.

1600 UTC, 1700 UTC, and 1800 UTC on 20 January 2007 were the times that were used for the sounding analyses. These times correspond to the time span forecasters expected TSSN to occur. Wichita Falls, TX was chosen as the sounding and time-section location because in the forecast discussion it was mentioned that in the area between northern Texas and southern Oklahoma temperature profiles showed cold enough

63
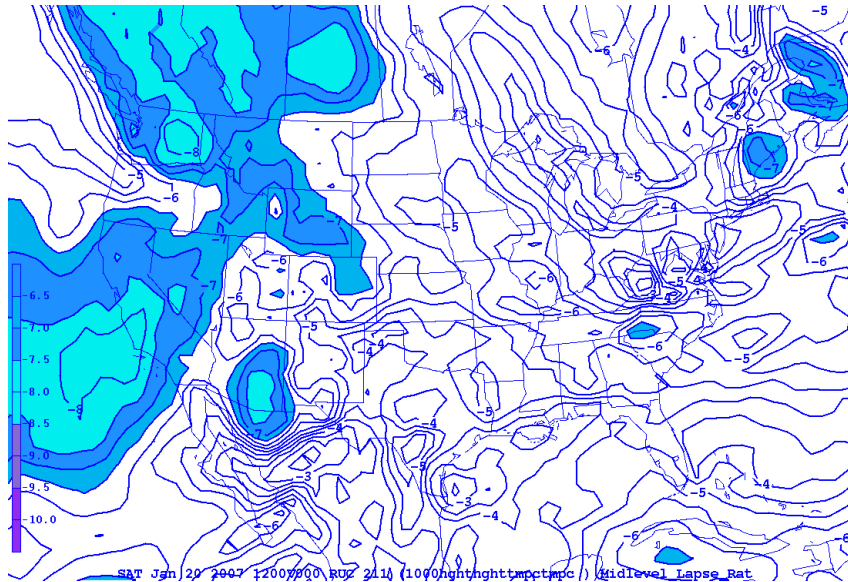
Figure 4.35 Lapse rates from the RUC initial fields for 700-mb to 500-mb (every $-1\ K\ km^{-1}$, solid with filled contours starting at $-6.5\ K\ km^{-1}$) for 20 January 2007 at 1200 UTC.

temperatures for lightning production and ample forcing for accent. Wichita Falls, TX is located in the area between northern Texas and southern Oklahoma.

Figure 4.36 is the 1600 UTC sounding from the RUC initial fields for Wichita Falls, TX on 20 January 2007. Refer to Figure 4.24 for the outlook map with the sounding location identified by a light blue star. The sounding reveals a mean relative humidity of 95% and a 700-mb to 500-mb lapse rate of $-4.4\ K\ km^{-1}$. The atmosphere is nearly saturated throughout most of the lower and middle troposphere and temperatures are below 0°C at the surface. However, there is a warm layer between 850-mb and 700-mb indicating that precipitation will fall as sleet instead of snow. Finally in the preferred lightning region between -10°C to -20 ° C (van den Broeke et al. 2005) the sounding appears stable. Analysis of this sounding reveals that TSSN development is not likely in the sounding region.
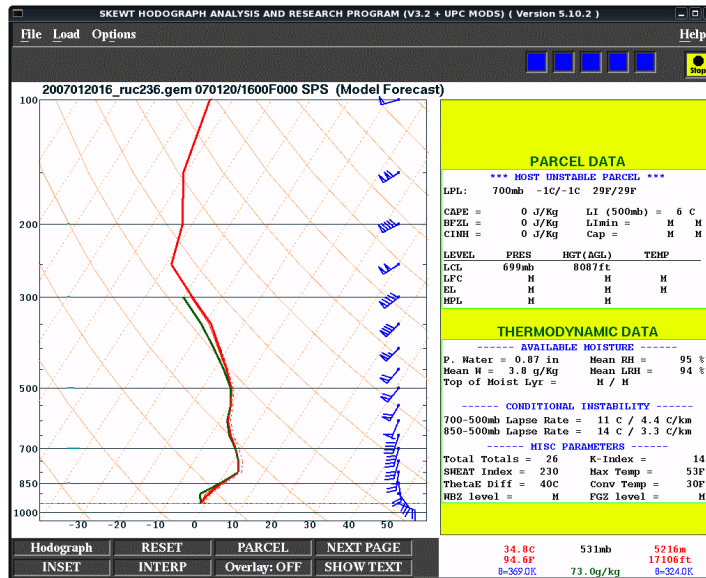
Figure 4.36 Sounding from the RUC initial fields for Wichita Falls, TX (KSPS), valid on 20 January 2007 at 1600 UTC.

Figure 4.37 is the 1700 UTC sounding from the RUC initial fields for Wichita Falls, TX on 20 January 2007. The main difference in this sounding is that there is 59 $J\ kg^{-1}$ of CAPE. 850-mb to 700-mb temperatures are still too warm and the sounding is still too stable in the preferred lightning region for TSSN development.

Figure 4.38 is the 1800 UTC sounding from the RUC initial fields for Wichita Falls, TX on 20 January 2007. There is no longer any CAPE present in this sounding and although the lapse rate is more unstable with a value of $-5.1\ K\ km^{-1}$ compared to a lapse rate of $-4.4\ K\ km^{-1}$ for the 1600 UTC, sounding temperatures are still too warm and it is still too stable in the preferred lightning region for TSSN development.
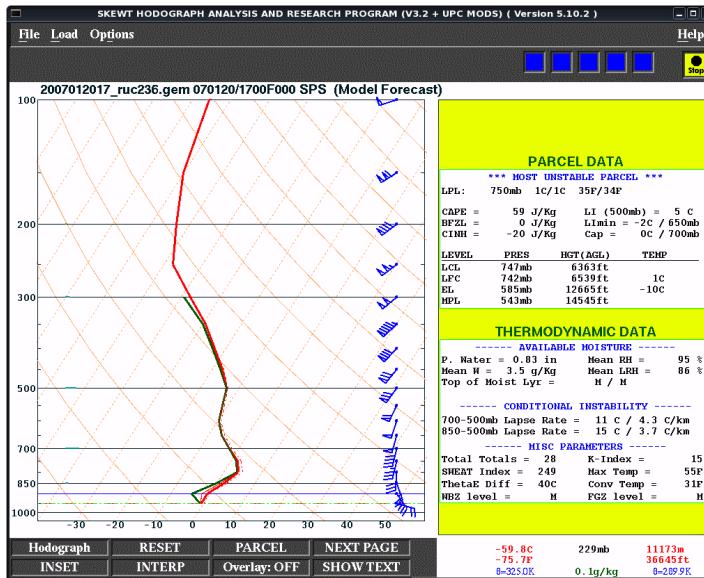
Figure 4.37 Sounding from the RUC initial fields for Wichita Falls, TX (KSPS), valid on 20 January 2007 at 1700 UTC.
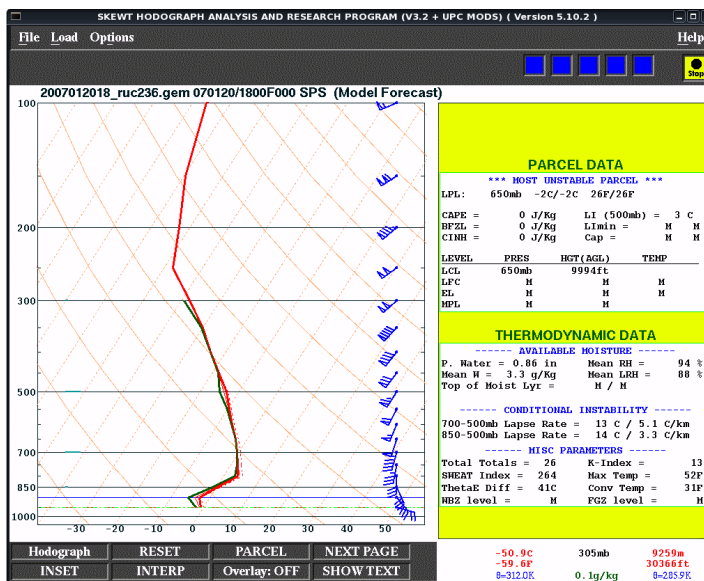
Figure 4.38 Sounding from the RUC initial fields for Wichita Falls, TX (KSPS), valid on 20 January 2007 at 1800 UTC.

The purpose of the following analyses is to demonstrate even more clearly the level of instability present with this event. Figure 4.39 is the space cross-section from Woodward, OK to Austin, TX for 20 Janaury 2007 at 1700 UTC. Refer to figure 4.24 for the location of the cross-section on the outlook map, which is identified by a black line. This cross-section line was chosen because it is drawn parallel to the thickness gradient and crosses near the sounding location of Wichita Falls, TX. 1700 UTC on 20 January 2007 was chossen for the cross-section time because the system was the most unstable at this time period. In this cross-section θ_e contours actually curve back over themselves between 850-mb and 600-mb. This signature is indicative of PI which if released will have a much faster convective growth rate, resulting in more upright convective towers.

Figure 4.40 is the time-section for Wichita Falls, TX from 0600 UTC 20 January 2007 through 0300 UTC 21 January 2007. Refer to Figure 4.35 for the time-section location on the outlook map, identified by a blue star. θ_e contours are diverging from each other with height especially between the hours of 1500 UTC and 1800 UTC further indicating the presence of PI in the atmosphere.
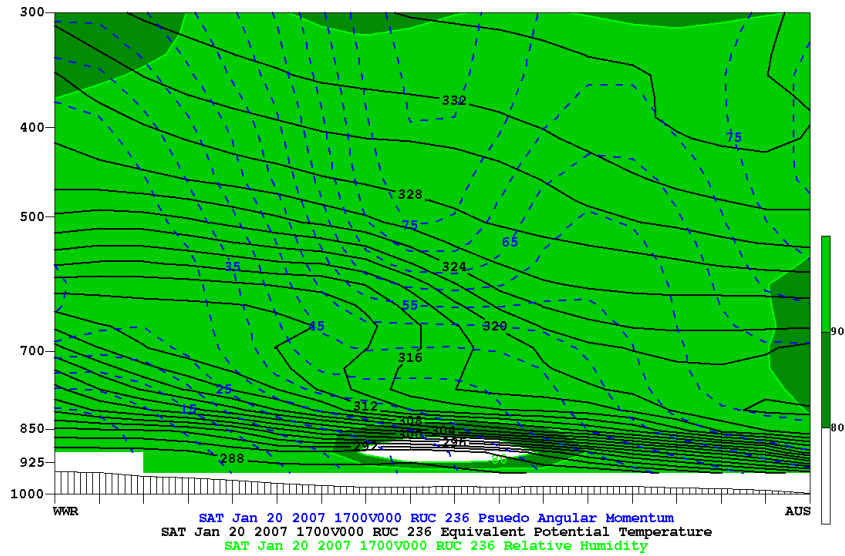
Figure 4.39 1000-mb to 300-mb space cross-section from the RUC initial fields of psuedo angular momentum (every 5 $kg\ m\ s^{-1}$, dashed blue lines), equivalent potential temperatures (every 2 K, solid black lines) and relative humidity (%, solid with filled contours that begin at 80%) from Woodward, OK to Austin, TX valid on 20 Janaury 2007 at 1700 UTC.

Figure 4.40 1000-mb to 400-mb time-section from the RUC initial fields with equivalent potential temperature (every 2 K, solid black lines) valid from 0600 UTC 20 January 2007 through 0300 UTC 21 January 2007 for Wichita Falls, TX. Time increases on the abscissa from right to left.

68

4.2.7 Remote Sensing Analysis

1202 UTC and 1145 UTC on 19 January 2007 was chosen for the radar and satellite analyses because they are the closest possible data times to 1200 UTC on 20 January 2007. The times for the radar and satellite analyses need to be close to 1200 UTC on 20 January 2007 to match with the synoptic analyses.

Figure 4.41 depicts base radar reflectivity for 20 January 2007 at 1202 UTC. The only precipitation falling in the outlook area for 1202 UTC on 20 January 2007 is mostly confined to Oklahoma. However, as the system tracks to the northeast, precipitation will spread into more of the forecast area. From the sounding analysis, precipitation for this event was mainly identified as sleet and not snow. Figure 4.42 depicts infrared satellite data from 20 January 2007 at 1145 UTC. The image displays cloud cover through most of the outlook area with cloud top temperatures of -50°C or colder in western Oklahoma and eastern Kansas.

SAT Jan 20 2007 1202 RADAR N0R 0. Deg (1km)
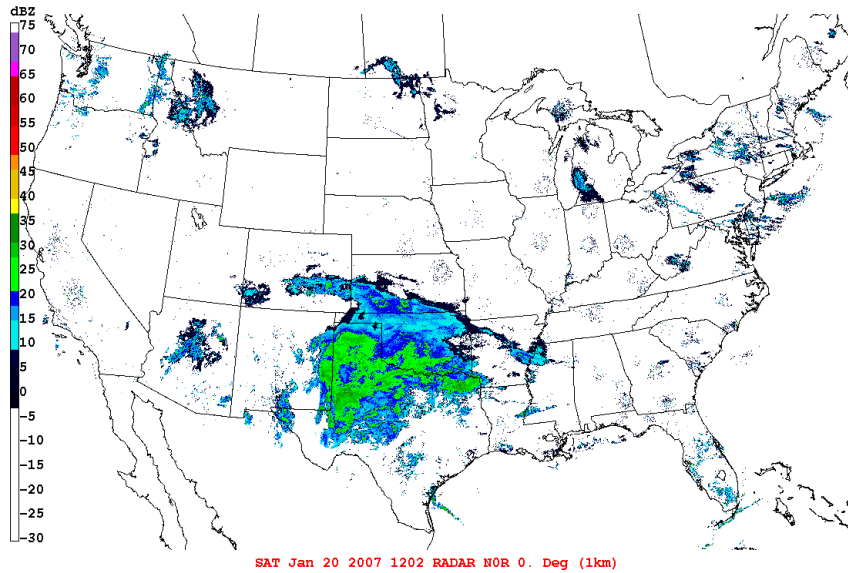
Figure 4.41 Base radar reflectivity for 20 January 2007 at 1202 UTC. The legend on the left is a color table, binned every 5 dBZ.

SAT Jan 20 2007 1145 GOES11 ch4 (FNm)
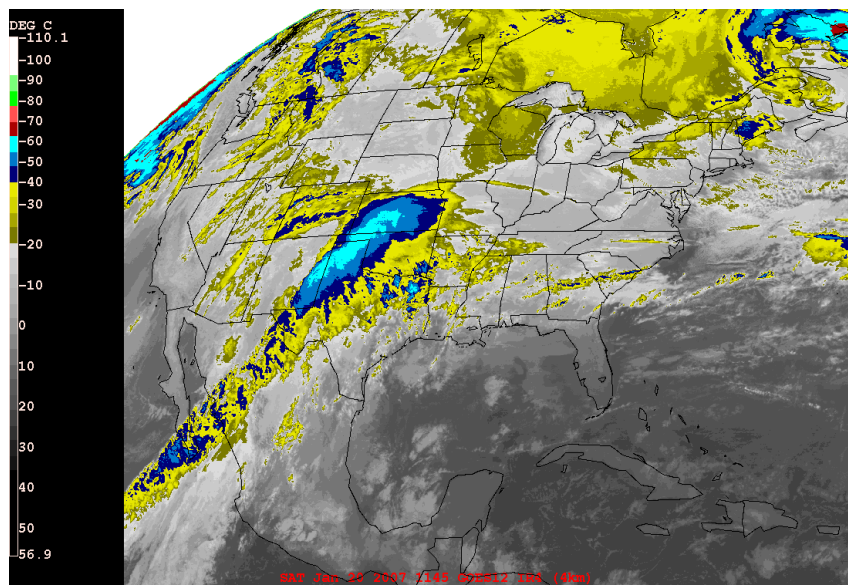
Figure 4.42 Infrared satellite imagery with color enhancement for 20 January 2007 at 1145 UTC. The legend on the left is a color table, binned every 10°C.

70

4.2.8   Banding Identification Analysis

Figure 4.43 shows a base radar reflectivity image from 20 January 2007 at 0924 UTC. 0924 UTC on 20 January 2007 was the time chosen for the banding analysis because at that time the base radar reflectivity shows some of the highest reflectivity during the event. In this image there is 35 dBZ reflectivity in southwestern Texas but this area does not meet the criteria for a precipitation band. After examining all the radar images from the event, it was determined that significant banding structure never developed in the outlook region.

4.2.9   Summary

The *ROCS* forecasters primarily used the GFS for the forecast of this event. The GFS indicated colder temperatures and weaker lapse rates would be present in the outlook region than actually occurred. This resulted in sleet with no lightning instead of TSSN. Since TSSN was forecasted to occur in the outlook region and did not occur this event is considered a "false alarm."

SAT Jan 20 2007 0924 RADAR N0R 0. Deg (1km)
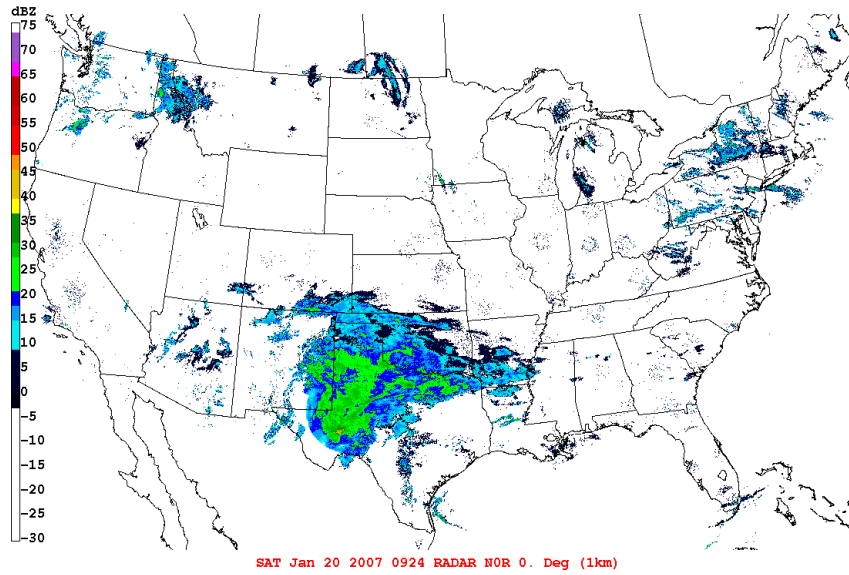
Figure 4.43 Base radar reflectivity for 20 January 2007 at 0924 UTC. The legend on left is a color table, binned every 5 dBZ.

4.3   13 February 2007 Case Study Analysis

4.3.1   Outlook & Forecast Discussion

The final event is the "missed" event that was forecasted for 1800 UTC on 12 February 2007 to 1800 UTC on 13 February 2007. TSSN was not expected to develop anywhere in the specified area of Figure 4.44. The outlook also included a forecast discussion outlining the decision not to issue a convective snow outlook. The complete forecast discussion is shown in Appendix C.

4.3.2   Analysis of Data from Original Forecast

To understand why the *ROCS* forecasters made their particular TSSN forecast decision it is important to look at the data they were using. The model used primarily by the forecasters for this event was the Global Forecast Model (GFS). In the forecast discussion issued by the *ROCS* group, convective snow was not expected to develop in the forecast domain because lapse rates were only around $-4.7\ K\ kg^{-1}$ and the best instability was expected to be in the warm sector of the system. They had no solid reason to think TSSN would develop. Figure 4.45 shows the location of a GFS model sounding from the data they were using to forecast. The location of the sounding is Des Moines, IA. Des Moines, IA was chosen for the analysis because the state of Iowa was specifically mention by the forecasters as containing weak forcing and lapse rates of only $-4.5\ K\ kg^{-1}$. Des Moines, IA is indentified with a purple triangle in Figure 4.45.
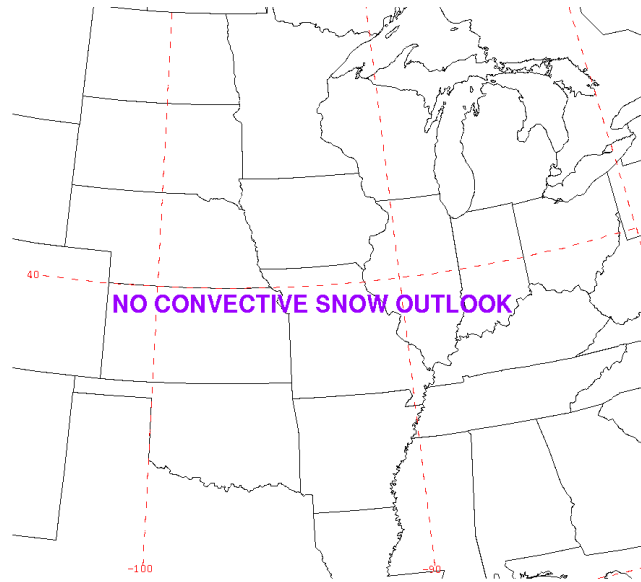
Figure 4.44 Indicates the lack of forecasted TSSN from 1800 UTC on 12 February 2007 to 1800 UTC on 13 February 2007 (created by the *ROCS* group).

Figure 4.45 Outlook map for 1800 UTC on 12 February 2007 through 1800 UTC on 13 February 2007. Olathe, KS (sounding and time-section location) is identified on the map using a light blue star. The cross-section line from Omaha, NE to Fort Smith, AR is identified on the map using a black line. Des Moines, IA (GFS sounding location) is identified on the map using a purple triangle.

74

Figure 4.46 is the GFS model sounding for Des Moines, IA on 13 February 2007 at 0600 UTC. 0600 UTC on 13 February 2007 was used as the sounding time because the forecast discussion specifically mentioned analyzing data for that time. The sounding shows ample moisture and temperatures cold enough for snow production but a weak lapse rate.

4.3.3 Outcome

Since convective snow was not expected to occur during this time period, it essential to look at the total event snowfall map and lightning data to determine if TSSN has occurred and in what region. The 72-hour total event snowfall map ending on 14 February 2007 at 1200 UTC (Fig. 4.47) shows that there is extensive snowfall throughout most of the upper Midwest with the heaviest snow fall in west central Illinois, Indiana, and Ohio.
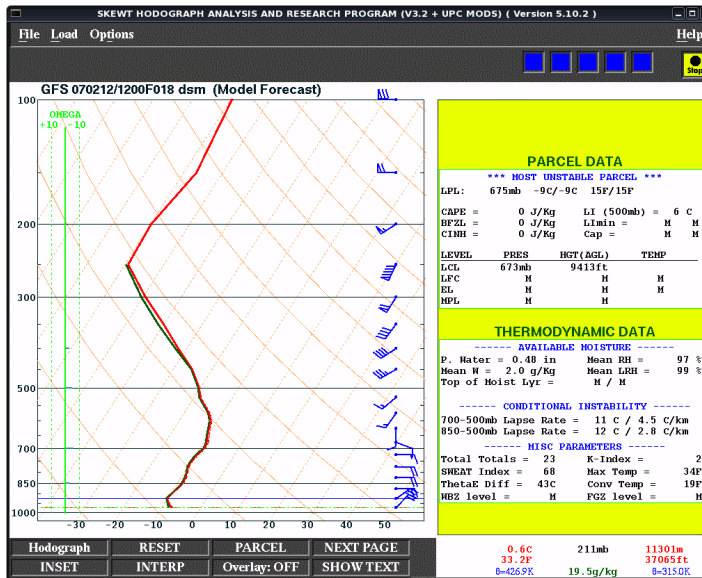
Figure 4.46 GFS 1200 UTC/18-hr forecast sounding for Des Moines, IA (KDSM) valid on 13 February 2007 at 0600 UTC.

072h COOP SNOWFALL ending at 20070214 1200 UTC
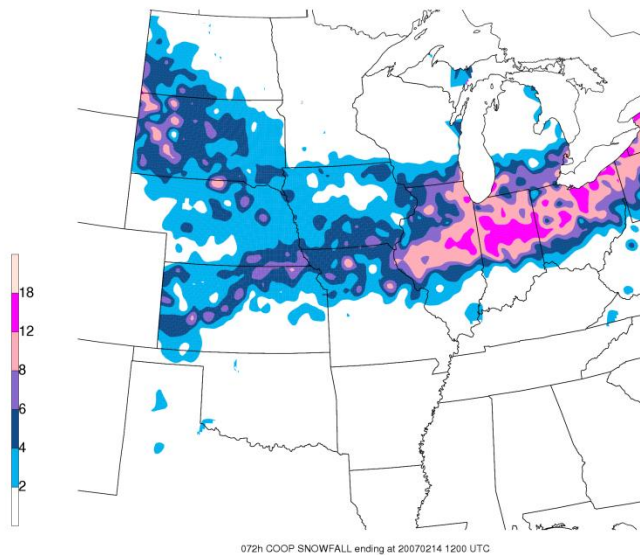
Figure 4.47 Total snowfall (every 2 in, filled contours starting at 2 in) map for 72-hours ending on 14 February 2007 at 1200 UTC (created by Chad Gravelle).

4.3.4 Lightning Data

Lightning flashes that occurred between 0500 UTC and 0600 UTC on 13 February 2007 are shown in Figure 4.48. This time period was chosen because it contained the greatest number of lightning flashes from the event. The lightning flashes are located in north-central and eastern Kansas and are associated with snowfall. In this event, the TSSN did not occur in the region with the highest snowfall. This event may thus be viewed as an outlier with respect to the Crowe et al. (2006) study.

4.3.5 Synoptic Analysis

All of the analyses for the mandatory synoptic levels are based off of the 0000 UTC RUC output for 13 February 2007. 0000 UTC on 13 February 2007 was chosen as the time for the synoptic analyses because this time bests depicts the system right before the TSSN activity actually occurred.

The surface analysis (Fig. 4.49) shows a 1004-mb low pressure center in northern Texas and Oklahoma. There is no specific outlook area to refer to for this event, so the focus will be on the location of the lightning strikes in Figure 4.48 and heavy snow in Figure 4.47. In the region consisting of Kansas, Missouri, Iowa, Illinois, Indiana, and Ohio, surface temperatures are cold enough or will become cold enough for measurable snowfall accumulation.
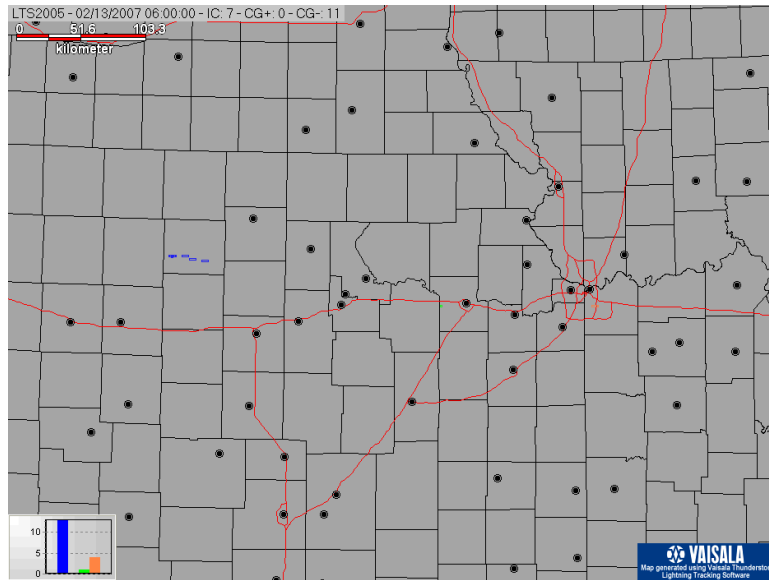
Figure 4.48 In-cloud (denoted by a dot) and cloud-to-ground (denoted by a negative or a positive sign) lightning flashes for 13 February 2007 between 0500 UTC and 0600 UTC. The graph on the bottom left side of the map displays the number of lightning flashes compared to the time they occurred. The time intervals are for every 10 minutes with the oldest lightning flashes being plotted on the far left of the graph and newest lighting flashes on the far right of the graph.
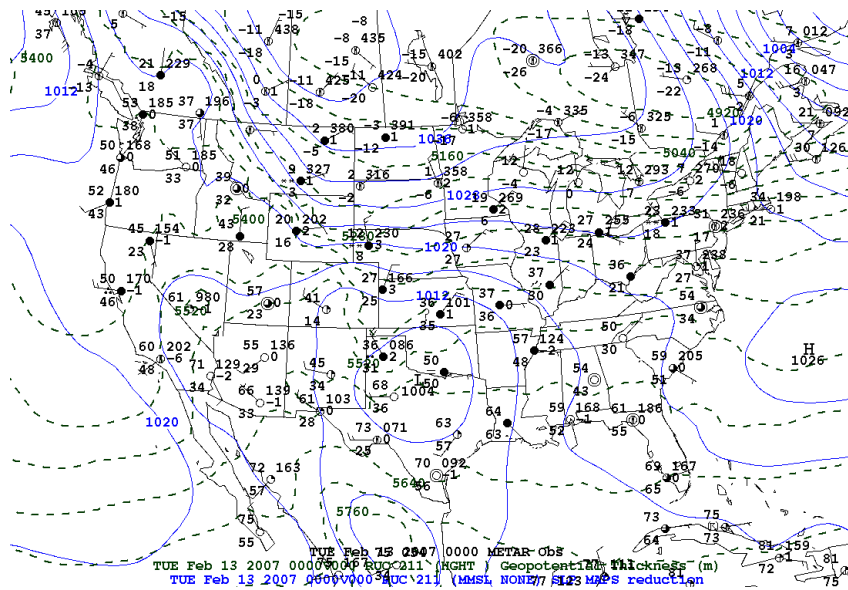
Figure 4.49 Surface analysis from the RUC initial fields with METAR observations in a standard station model configuration (black), geopotential thicknesses (every 60 gpm, dashed green lines) and mean sea level pressures (every 4 mb, solid blue lines) for 13 February 2007 at 0000 UTC.

The 850-mb analysis (Figure 4.50) displays some WAA and CAA but with rather large solenoids the advections appear to be very weak. The system does not appear organized. The 700-mb analysis (Figure 4.51) shows a well defined trough with a slight negative-tilt associated with it, indicating the system is still developing and intensifying. There may also be a slight TROWAL signature through eastern Nebraska, eastern Kansas, and western Missouri. WAA and CAA still appear weak at this level. The 500-mb analysis (Figure 4.52) depicts a minor vorticity maximum located in northern Texas. This small amount of CVA does suggest some upward vertical motion, which helps develop more convergence at the surface and divergence aloft.

The 300-mb analysis (Figure 4.53) depicts a strong jet maxima with winds of 140 kts located off the coast of California. As this jet streak moves into the United States it will likely increase divergence which will help to enhance upward vertical motion in northern New Mexico, northwestern Texas, Kansas, Missouri, and any other location that happens to be on the left-front quadrant of the jet streak.
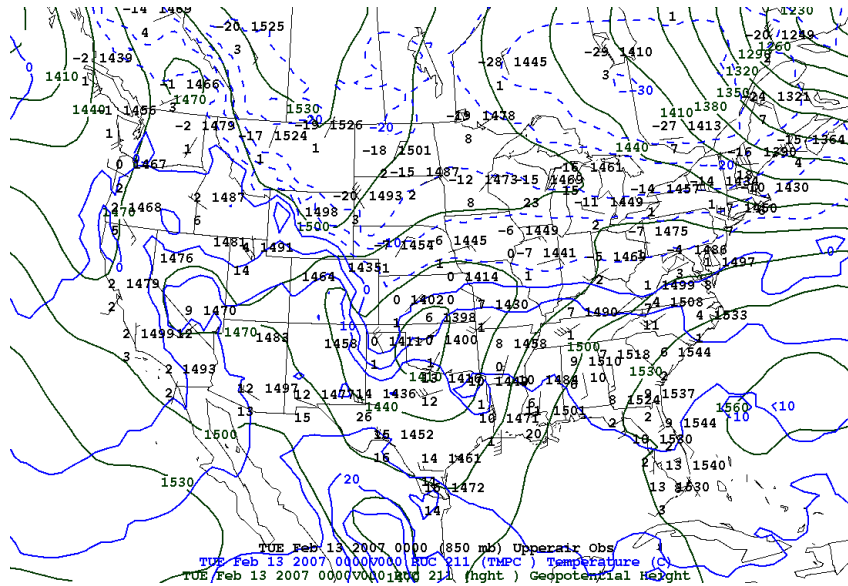
Figure 4.50 Analysis from the RUC initial fields for 850-mb with upper-air station models (black), temperatures (every 5 Cº, solid and dashed blue lines) and geopotential heights (every 30 gpm, solid green lines) for 13 February 2007 at 0000 UTC.
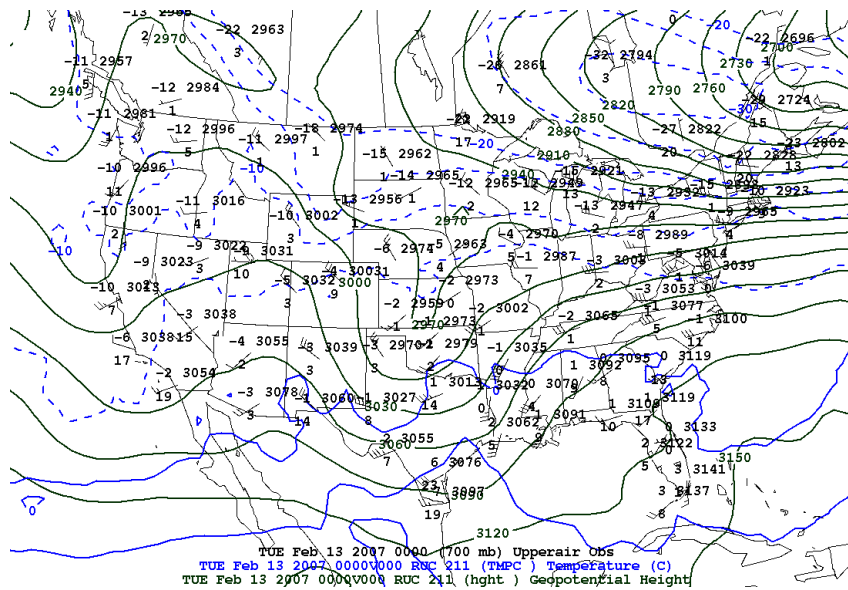
Figure 4.51 Analysis from the RUC initial fields for 700-mb with upper-air station models (black), temperatures (every 5 Cº, solid and dashed blue lines) and geopotential heights (every 30 gpm, solid green lines) for 13 February 2007 at 0000 UTC.
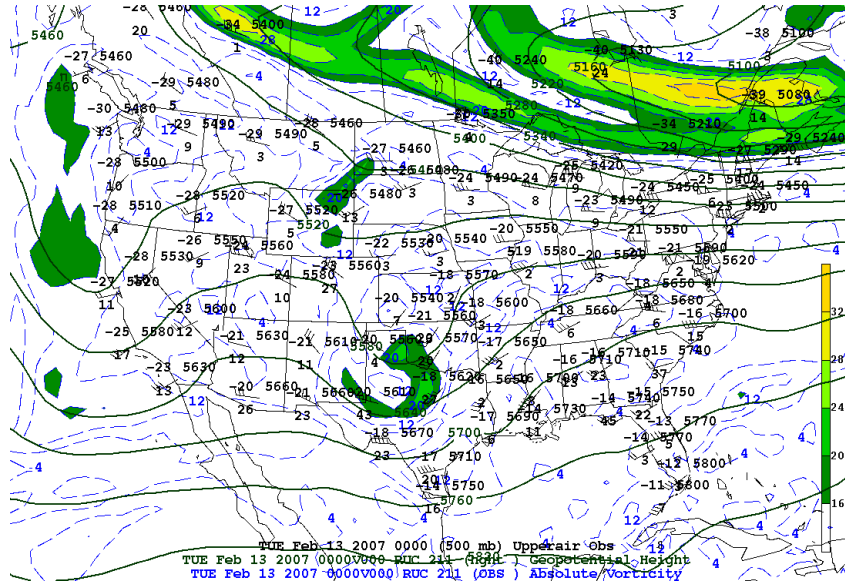
Figure 4.52 Analysis from the RUC initial fields for 500-mb with upper-air station models (black), geopotential heights (every 60 gpm, solid green lines), and absolute vorticity ($1 \times 10^{-5}\ s^{-1}$ with an interval of $4 \times 10^{-5}\ s^{-1}$, solid with filled contours that begin at $16 \times 10^{-5}\ s^{-1}$) for 13 February 2007 at 0000 UTC.
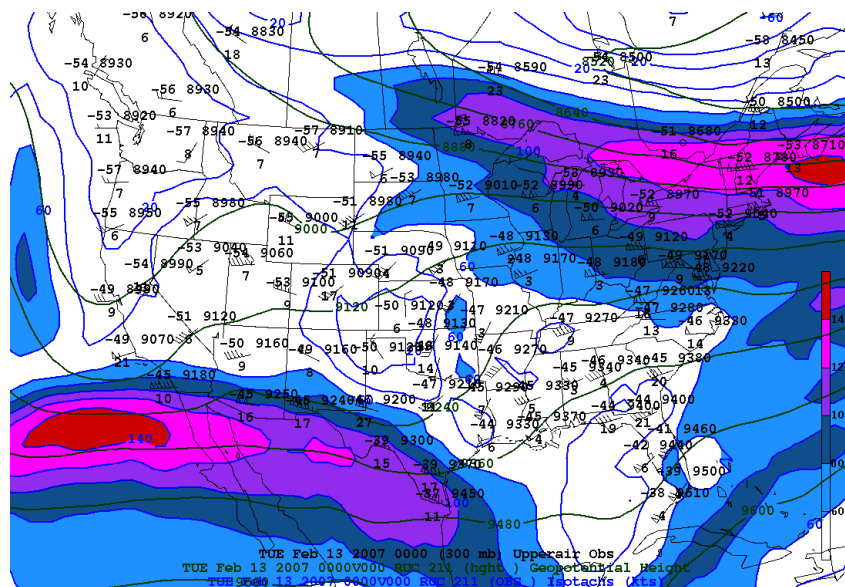
Figure 4.53 Analysis from the RUC initial fields for 300-mb with upper-air station models (black), geopotential heights (every 120 gpm, solid green lines), and isotachs (every 20 kts, shaded contours over 60 kts) for 13 February 2007 at 0000 UTC.

81

Figure 4.54 depicts relative humidity from 950-mb to 500-mb. All of the areas that received snowfall and/or lightning had ample moisture with relative humidities of 80% or greater.

Figure 4.55 depicts Q-vector divergence which indicates locations of mid-level forcing for ascent. This then gives us an idea about the vertical motion in that location. There are good sources of Q-vector divergence in Kansas, Iowa, Illinois, Indiana, and Ohio giving good indication that there is decent force for accent in those areas.

Figure 4.56 is the thickness analysis. The rain/snow line cuts through Illinois, Indiana, and Ohio where the most snowfall occur.
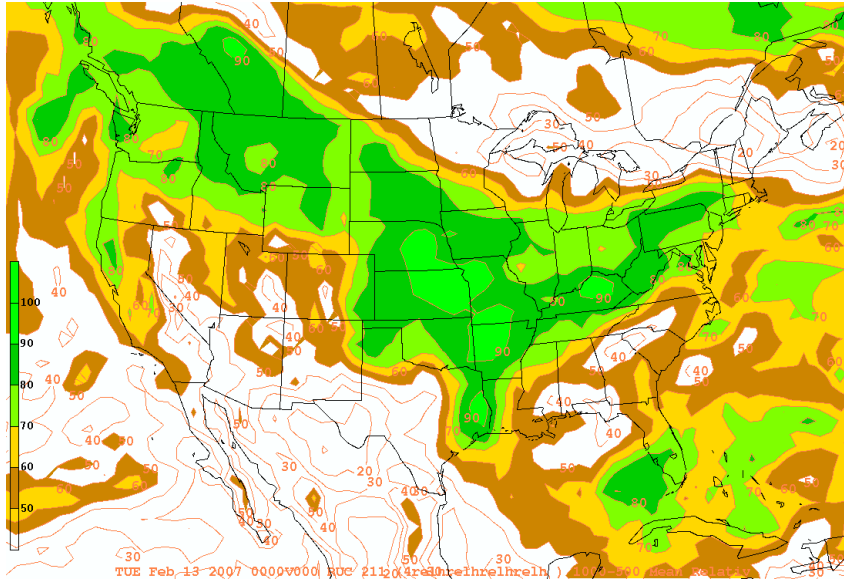
Figure 4.54 Relative humidity from the RUC initial fields (%, solid with filled contours that begin at 50%) for 950-mb to 500-mb for 13 February 2007 at 0000 UTC.
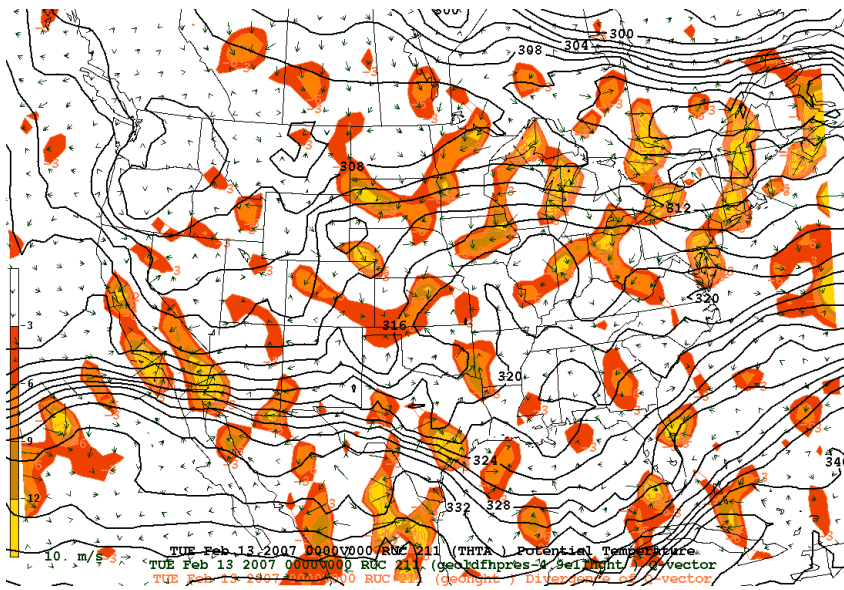
Figure 4.55 700-mb to 300-mb Q-vector divergence from the RUC initial fields ($m \ kg^{-1} \ s^{-1}$ with an interval of $-3 \times 10^{-16} \ m \ kg^{-1} \ s^{-1}$ solid and filled), 700-mb to 300-mb Q-vectors from the RUC initial fields (green arrows) and 500-mb potential temperatures from the RUC initial fields (every 2 K, solid black lines) for 13 February 2007 at 0000 UTC.
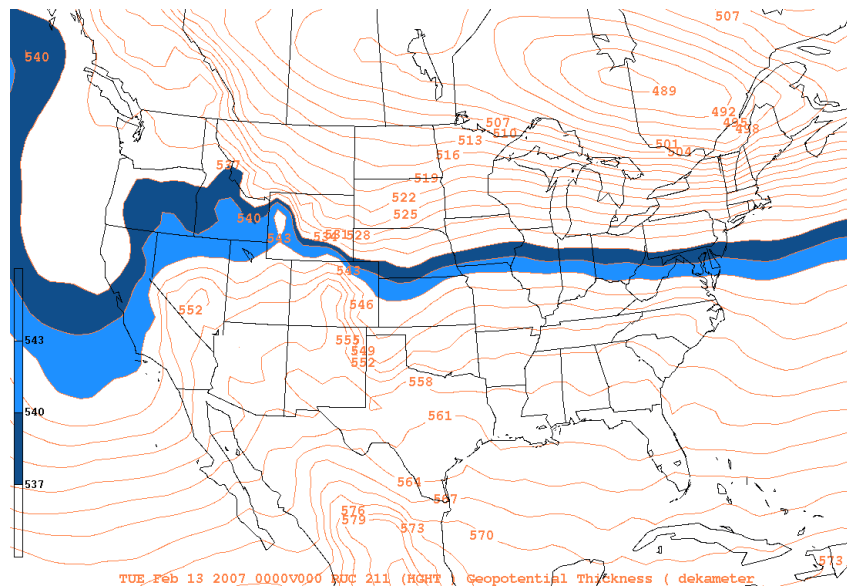
Figure 4.56 Geopotential thickness from the RUC initial fields for 1000-mb to 500-mb (every 3 dam, solid with filled contours starting at 537 dam) for 13 February 2007 at 0000 UTC.

4.3.6   Mesoscale & Synoptic Analysis

Figure 4.57 is the lapse rate analysis from 700-mb to 500-mb for 13 February 2007 at 0000 UTC. Lapse rates in the areas that received snow and/or lightning have lapse rates from $-5.5\ K\ kg^{-1}$ to $-6.5\ K\ kg^{-1}$. These lapse rates are reasonable for TSSN development (Market et al. 2006) as long as there is sufficient moisture and a strong enough lifting mechanism to enable the release of instability.

Refer to Figure 4.45 for the no convective snow outlook from 1800 UTC on 12 February 2007 through 1800 UTC on 13 February 2007. It shows the locations of the sounding, time-section, GFS sounding, and cross-section line. 0200 UTC, 0400 UTC, and 0600 UTC for 13 February 2007 are the times used for the sounding analyses because they correspond to the time frame when TSSN was occurring. 0400 UTC on 13

84

February 2007 best depicts the environment that TSSN is occurring. 0400 UTC on 13 February 2007 is also used for the cross-section analysis. Olathe, KS (KIXD) was used as the soundings and cross-section location because it is located in close proximity to the TSSN activity.

Figure 4.58 is the 0200 UTC sounding from the RUC initial fields for Olathe, Kansas (KIXD) on 13 February 2007. The sounding depicts relative humidity of 87%, a lapse rate of $-6.5 \ K \ kg^{-1}$, low-level temperatures are just under 0°C, and the sounding approaches moist neutral in the preferred lighting region between -10°C and -20°C (van den Broeke et al. 2005). From this sounding alone, TSSN development certainly appears possible.

Figure 4.59 is the 0400 UTC sounding from the RUC initial fields for Olathe, Kansas (KIXD) on 13 February 2007. The main difference in 0400 UTC sounding from the 0200 UTC sounding is that there is $2 \ J \ kg^{-1}$ of CAPE with the 0400 UTC sounding. This value of CAPE is too small by either van den Broeke et al. (2005) or Market et al. (2006), but it is present and positive none the less. Relative humidity increases to 90% and the lapse rate becomes more conducive to TSSN at $-6.8 \ K \ kg^{-1}$.

Figure 4.60 is the 0600 UTC sounding from the RUC initial fields for Olathe, Kansas (KIXD) on 13 February 2007. The 0600 UTC sounding differs from the 0400 UTC sounding due to the fact that CAPE is no longer present, the lapse rate is slightly larger ($-6.7 \ K \ kg^{-1}$), and the relative humidity drops back down to 87%.
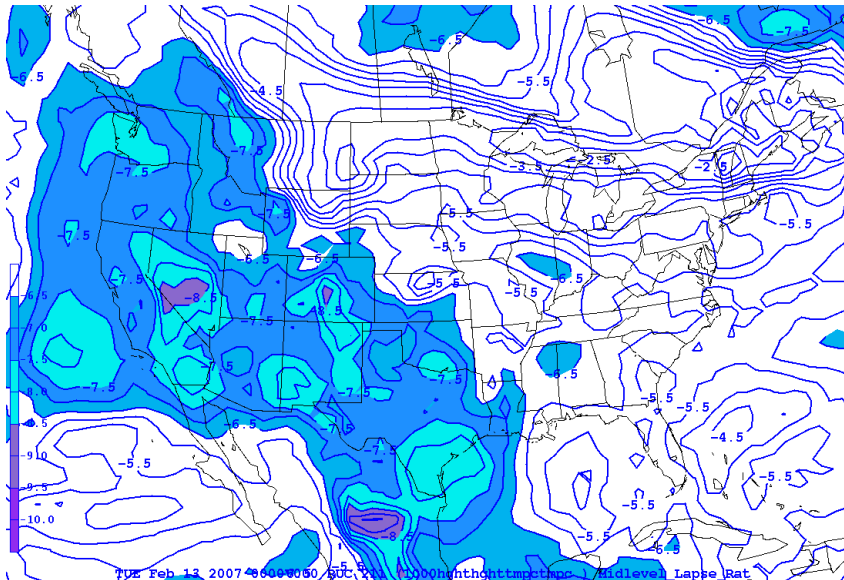
Figure 4.57 Lapse rates from the RUC initial fields for 700-mb to 500-mb (every $-1\ K\ km^{-1}$, solid with filled contours starting at $-6.5\ K\ km^{-1}$) for 13 February 2007 at 0000 UTC.
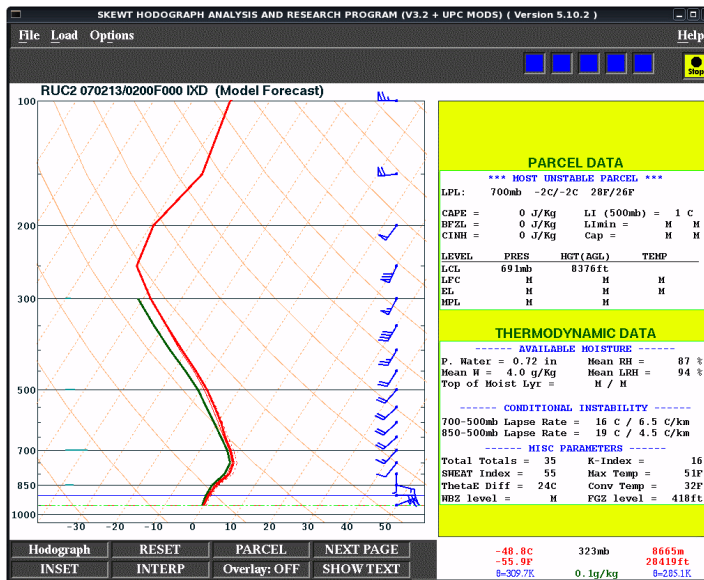
Figure 4.58 Sounding from the RUC initial fields for Olathe, KS (KIXD) valid on 13 February 2007 at 0200 UTC.
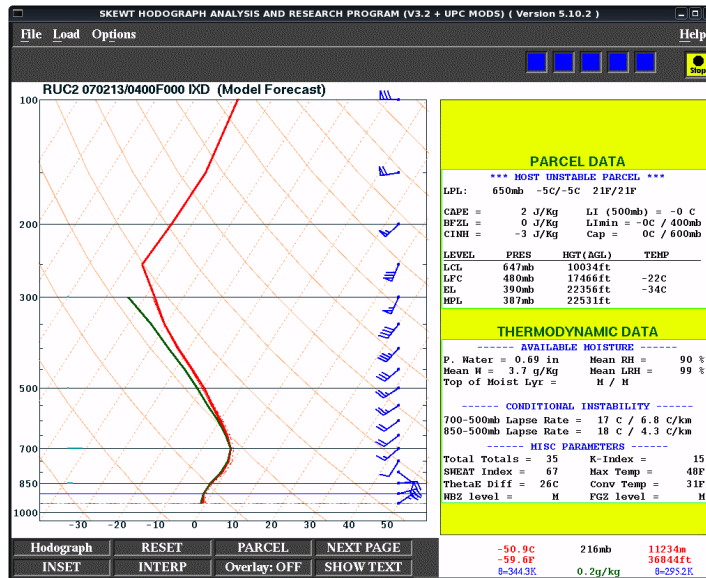
Figure 4.59 Sounding from the RUC initial fields for Olathe, KS (KIXD) valid on 13 February 2007 at 0400 UTC.

Figure 4.61 is the space cross-section from Omaha, NE to Fort Smith, AR for 13 February 2007 at 0400 UTC. This cross-section line was chosen because it is drawn parallel to the thickness gradient and intersects near the sounding location of Olathe, KS (KIXD). In the space cross-section there is a large region between 700-mb and 400-mb where the θ_e contours are becoming more widely separated indicating increasing instability in that region of the atmosphere.

Figure 4.62 is the time-section from 0000 UTC on 13 February 2007 through 0800 UTC 13 on February 2007 for Olathe, KS. Refer to figure 4.45 for the location of the time-section on the outlook map for 1800 UTC on 12 February 2007 through 1800 UTC on 13 February 2007. The location is identified by a light blue star. As with the cross-section, in the region between 700-mb to 400-mb the θ_e contours are vertical, or nearly so, if they exist at all, suggesting a deep, persistent layer of potential instability over Olathe, KS (KIXD).
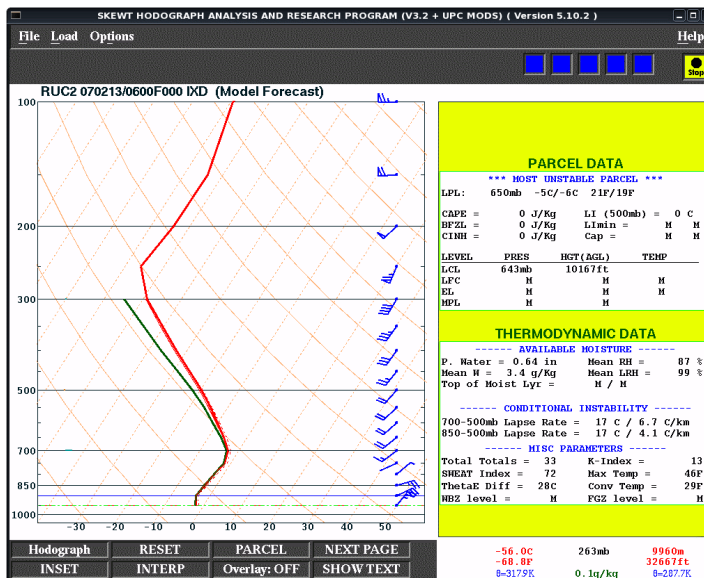
Figure 4.60 Sounding from the RUC initial fields for Olathe, KS (KIXD) valid on 13 February 2007 at 0600 UTC.
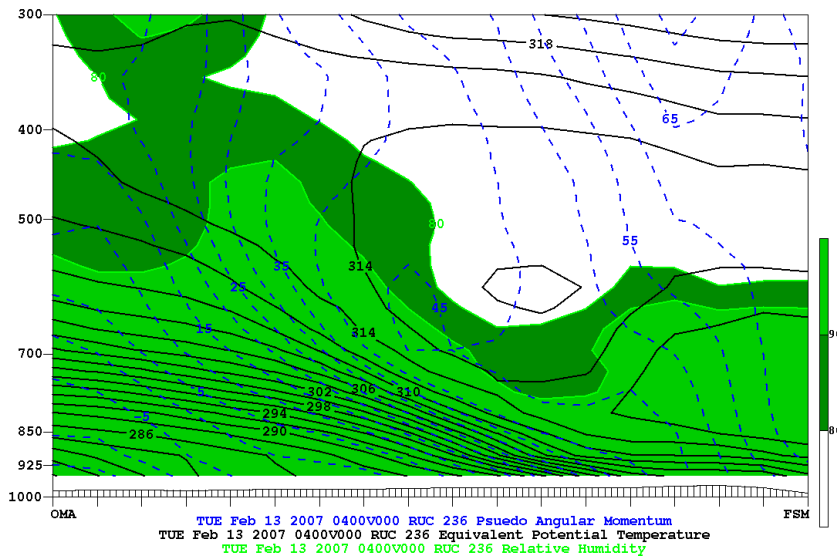
Figure 4.61 1000-mb to 300-mb space cross-section from the RUC initial fields of psuedo-angular momentum (every 5 $kg\ m\ s^{-1}$, dashed red lines), equivalent potential temperatures (every 2 K, solid black lines), and relative humidity (%, solid with filled contours that begin at 80%) from Omaha, NE to Fort Smith, AR valid on 13 February 2007 at 0400 UTC.
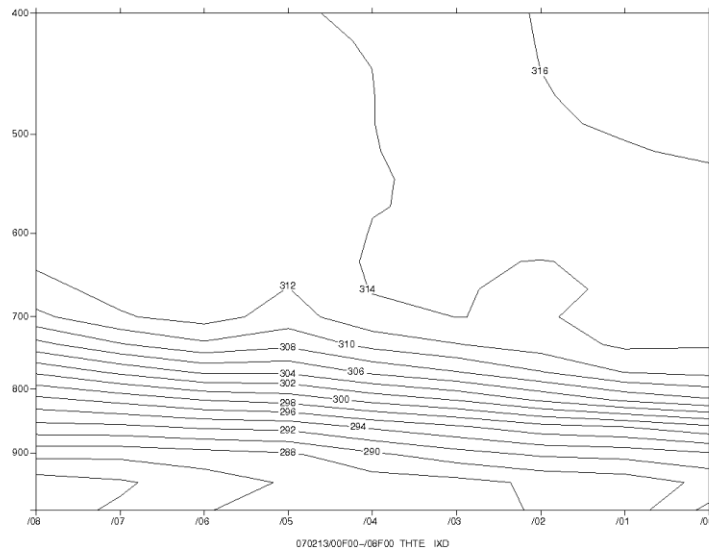
Figure 4.62 1000-mb to 400-mb time-section from the RUC initial with equivalent potential temperatures (every 2 K, solid black lines) from 0000 UTC on 13 February 2007 through 0800 UTC on 13 February 2007 for Olathe, KS. Time increases on the abscissa from right to left.

4.3.7   Remote Sensing Analysis

0002 UTC and 0015 UTC on 13 February 2007 was chosen for the radar and satellite analyses because they are the closest possible data times to 0000 UTC on 13 February 2007. The times for the radar and satellite analyses need to be close to 0000 UTC to match with the synoptic analyses.

Figure 4.63 is base radar reflectivity for 13 February 2007 at 0002 UTC. In Figure 4.63 there is a very strong radar signature for this event detailing the locations of the wrap-around structure (located in northern Kansas and Missouri), the dry slot (located in southern Kansas and Oklahoma), and the structure of the fronts associated with the parent extratropical cyclone. From the base radar reflectivity we can see that northern Kansas, Missouri, southern Illinois, southern Indiana, and southern Ohio are all experiencing

89

precipitation. From the sounding and thickness analysis we can say that the precipitation is in the form of snowfall.

Figure 4.64 depicts infrared satellite data from 13 February 2007 at 0015 UTC. The image displays cloud cover through most of Kansas, Missouri, Illinois, Indiana, and Ohio. Cloud tops associated with snowfall and temperatures of -60°C or less are located in northeastern Kansas and southwestern Nebraska. The colder cloud tops are in the regions where lightning activity took place. There may possibly be a connection between lightning development and cloud top temperatures.

4.3.8   Banding Identification Analysis

0048 UTC on 13 February 2007 was the time chosen for the banding analysis because at that time the base radar reflectivity shows some of the highest reflectivity during the event.

Figure 4.65 shows base radar reflectivity from 13 February 2007 at 0048 UTC with a cold-frontal band embedded in weaker reflectivity echoes. In this image there is a band of 50 dBz reflectivity (on the southeast border of Texas) located near the cold-front that has persisted for at least two hours and is at least 300 km long and 10-50 km wide. Although this is technically a radar reflectivity band, it is occurring as non-frozen precipitation and has no bearing on TSSN development. There are no banding structures located in the regions receiving snowfall.
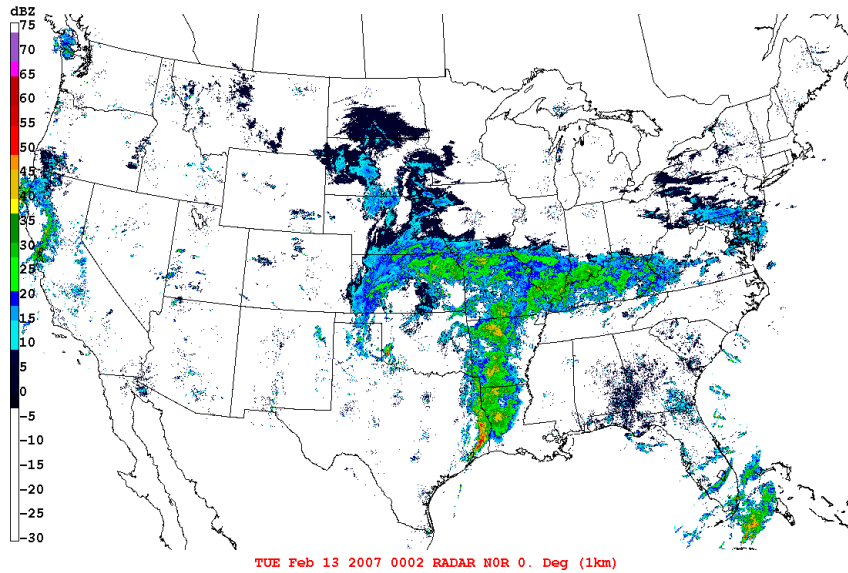
Figure 4.63 Base radar reflectivity for 13 February 2007 at 0002 UTC. The legend on the left is a color table, binned every 5 dBZ.
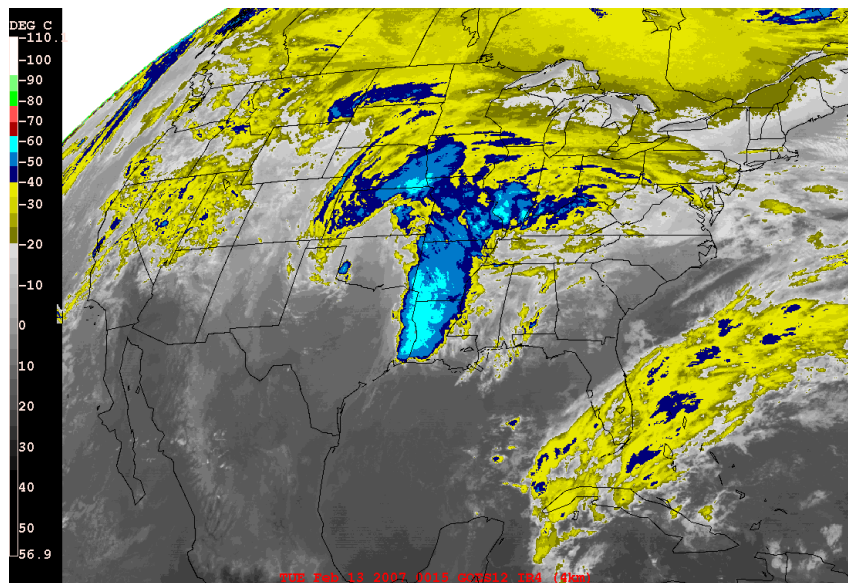
Figure 4.64 Infrared satellite imagery with color enhancement for 13 February 2007 at 0015 UTC. The legend on the left is a color table, binned every 10°C.

91
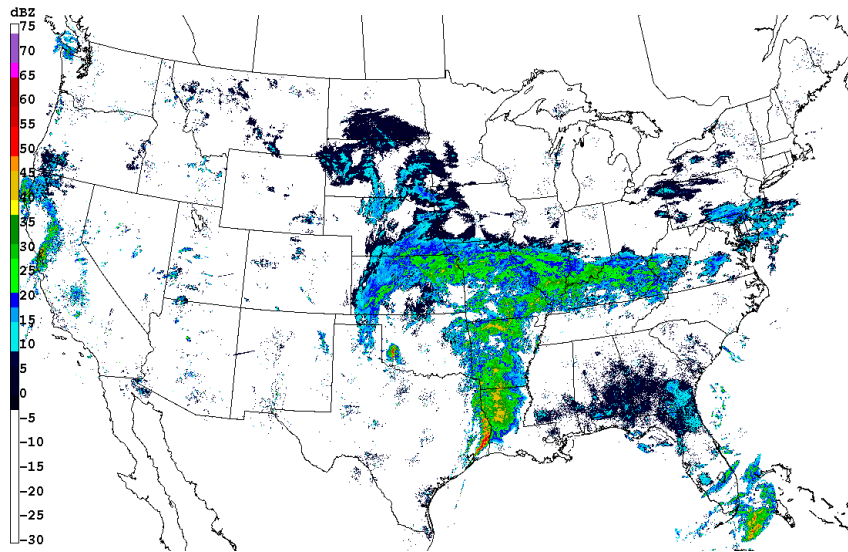
Figure 4.65 Base radar reflectivity for 13 February 2007 at 0048 UTC. The legend on the left is a color table, binned every 10°C.

4.3.9   Summary

The *ROCS* forecasters primarily used the GFS for the forecasting of this event.

During this event temperatures were cold enough for snow production, the system

possessed sufficient moisture, and there was ample forcing for accent. From sounding

analysis it was determined that thermal profiles approached moist neutral during the

event and there was instability in the preferred lightning region between -10°C and -20°C

(van den Broeke et al. 2005). Model solutions indicted warmer temperatures and weaker

lapse rates than actually occurred. Due to the model solutions the *ROCS* forecasters

believed that convective snow would not occur in the forecast domain. Since TSSN

developed this event became a "missed" forecast event.

Chapter 5   Verification of Forecasts

For each season from 2004 to 2007 verification statistics for the day 1 outlooks and day 2 outlooks were performed and threat scores (TS) were calculated. The TS shows the improvement of the forecasts over time. Table 5-1 shows the data for day 1 outlooks from each season. The table lists each season, the number of hits, false alarms, misses, the total forecasts, and finally the calculated threat score. The threat score will range from 0 to 1 with 1 being the best possible score. Figure 5.1 is a graph showing the threat scores from each season. Starting with the 2004 season it is an apparent that there is an increase in the TS as time goes forward indicating that the forecasting skill is improving with each season. There is a drop in the TS for Season 2007 but this season is considered an outlier because the *ROCS* project was being concluded. With student forecasters graduating the forecasting sessions were suspended on 31 January 2008, thus shortening the season.

Seasons	Hits	False Alarms	Misses	Totals	TS
2003-2004	4	18	7	29	0.14
2004-2005	10	16	12	38	0.26
2005-2006	11	14	8	33	0.33
2006-2007	12	4	10	26	0.46
2007-2008	7	3	6	16	0.44
Day 1 Outlooks					
Best Score =1					

Table 5-1 Data table listing all of the *ROCS* forecasted seasons from 2003 to 2008 with the total number of day 1 "hits," "false alarms," and "missed" events for each season along with the calculated TS.
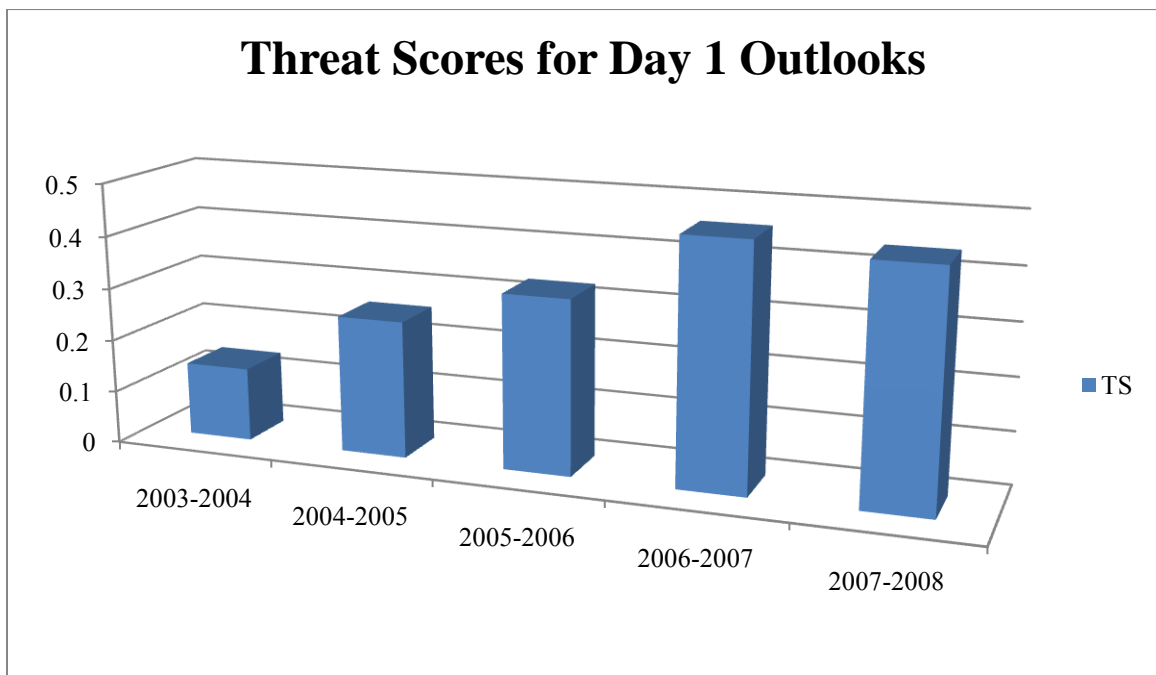
5.1 Graph listing the day 1 threat scores for each *ROCS* season from 2004-2007.

Table 5-2 shows the data for day 2 outlooks from each season. The table lists each season, the number of hits, false alarms, misses, the total forecasts, and finally the calculated threat score. The threat score will range from 0 to 1 with 1 being the best possible score. Figure 5.2 is a graph showing the threat scores from each season. Starting with the 2004 season it is an apparent that there is an increase in the TS as time goes forward indicating that the forecasting skill is improving with each season just as with the day 1 outlooks. There is also a drop in the TS for Season 2007 but again this season is considered an outlier because the *ROCS* project was being concluded. With student forecasters graduating the forecasting sessions were suspended on 31 January 2008, thus shortening the season.

There are many possibilities on why the *ROCS* forecasters improved in their forecasting skill throughout the project. Probably the two biggest factors to that improvement was the increased experience with forecasting TSSN and the applying of knowledge about TSSN development from research findings. To a lesser extent changes in large-scale patterns may have influenced the TS in various seasons. It has to be noted that when using TS for forecast verification the amount of events in a season can skew the results. This has to be taken in account when comparing TS between different seasons.

Seasons	Hits	False Alarms	Misses	Totals	TS
2003-2004	1	22	5	28	0.04
2004-2005	3	21	7	31	0.10
2005-2006	7	14	8	29	0.24
2006-2007	8	7	6	21	0.38
2007-2008	4	1	9	14	0.29
Day 2 Outlooks					
Best Score =1					

Table 5-2 Data table listing all of the *ROCS* forecasted seasons from 2003 to 2008 with the total number of day 2 "hits," "false alarms," and "missed" events for each season along with the calculated TS.
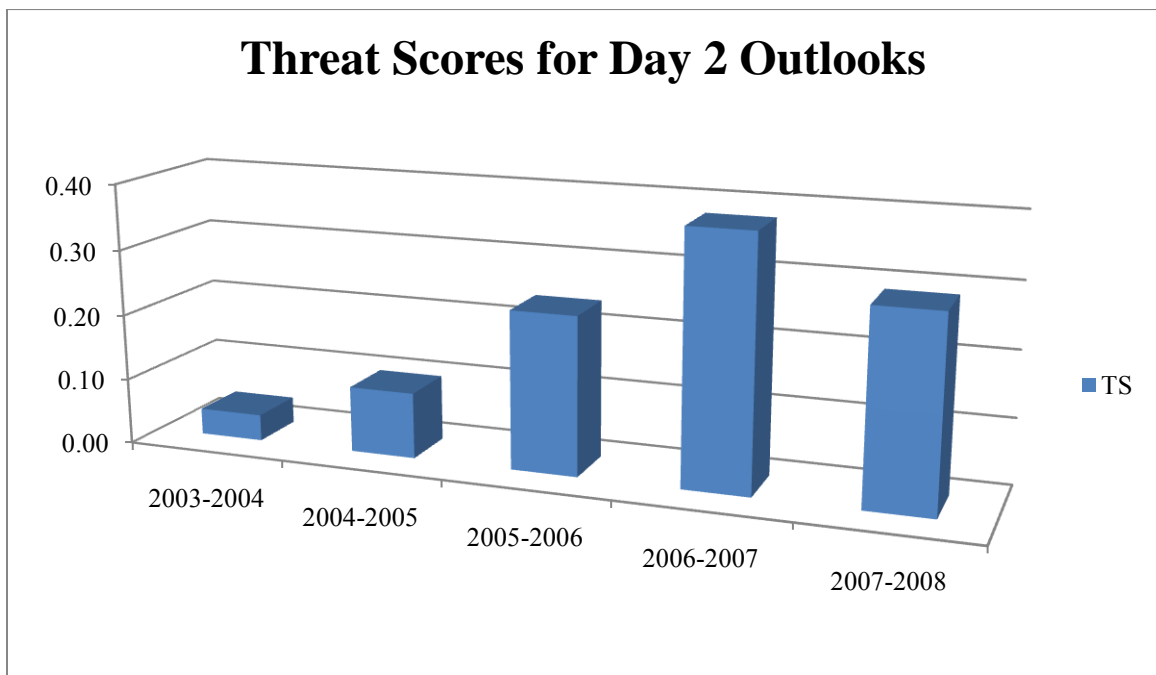

5.2 Graph listing the day 2 threat scores for each *ROCS* season from 2003-2008.

Chapter 6 Summary & Conclusions

After the analysis of the three forecast events, a few important conclusions can be made. All three of the events were associated with a mid-latitude cyclone that was fairly weak with low pressures remaining above 1000-mb during the height of the event. For each of the events there was adequate forcing for ascent, and ample moisture in at least part of the outlook area. The main differences between the three cases end up being the temperature and stability profiles.

For the "hit" event, temperatures remained in the range for snow production and lapse rates were between -4 °C km^{-1} to -6 °C km^{-1}. Even though the lapse rates were not substantial, the atmosphere became unstable enough (on scales below what the RUC can resolve) for convection and lightning production. The forecasters had reliable model data from the GFS, WRF, MASS-KF, and MASS-Grell models and were able to produce a successful forecast.

The "false alarm" event was not as clear cut at the "hit" event. Model output from the GFS and the WRF indicated temperatures would be cold enough for snow production in the outlook area, but during the actual event a warm pocket between 900-mb and 700-mb enabled sleet production instead of snow. Also, with the development of this warm pocket the atmosphere ended up being too stable in the preferred lightning region between -10°C and -20°C (van den Broeke et al. 2005). In the case of this event, the GFS indicated colder temperatures than actually occurred. That is the reason why the forecast ended up as a "false alarm."

For the "missed" event the GFS as well as the NAM and the WRF were used for the forecast. Model output indicted that lapse rates would be very weak for the event with the lowest value being only -4.5 °C km^{-1}. Forecasters determined that with such weak atmospheric instability no convective snow would occur anywhere in the forecast region. Again, the model output was incorrect for the event and actual lapse rates reached -6.8 °C km^{-1}.

From the analysis of these three cases it is apparent that when forecasting TSSN if adequate moisture and a lifting mechanism are present then the temperature profiles must be examined closely to determine if snow development is possible and the instability of the system must be analyzed correctly for an accurate forecast. Unfortunately, even if model solutions are interpreted accurately, the model may not produce accurate solutions. This is especially true for the location and release of instability.

From calculating the TS for day 1 and day 2 outlooks for the five TSSN seasons that were forecasted by the *ROCS* group, it was determined that with each progressing season the *ROCS* forecasters improved their forecasting skills. This indicates that with the research being conducted on TSSN and their experience from previous events, the forecasters were able to produce better forecasts as time went on. Experience with forecasting TSSN lead to better forecasts because the forecasters became familiar with the intricacies of TSSN and were able to learn from their forecasting mistakes. Research preformed on TSSN improved forecasts because it provided valuable knowledge to the forecasters on how TSSN develops and what to look for in model solutions. Hopefully the analysis on these three TSSN events and the calculation of the TS can help forecasters

in the future predict TSSN with better accuracy and to understand the development of

TSSN more fully.

Appendix A

The following is the original TSSN forecast discussion written by *ROCS*

forecasters for 1800 UTC 30 November 2006 through 01 December 2006:

Day 1 - Forecast valid from 1800 UTC 30 November to 1800 UTC 01 December 2006

WV loops depict organizing area of moisture over N TX, W OK, and S KS this morning ahead of positively tilted mid-level trof. Powerful vort max near base of trof over W TX panhandle at 12Z, with significant 700-300 mb Q convergence centered on PPA (downstream, over N TX panhandle) on western edge of burgeoning moisture area. Morning radar summaries depict expanding area of precipitation over W OK, with banding structures already apparent west of the nascent low near Texarkana. 12Z/30 GFS solutions dominate this outlook, as the best run-to-run continuity has emerged over the last 12-18 hrs with that platform. Some support also comes from the 12Z/30 NAM, 00Z/30 runs from the in-house WRF and MASS-KF and MASS-Grell models, and a peek at the 15Z/30 RUC output. Largely a continuation of yesterday's outlook for this period. Region of best ingredients for TSSN is on the move, appearing near the intersection of the trowal axis, and the the axis of the emerging dry slot a la Nicosia and Grumm. 700- to 600-mb frontogenesis in presence of deep moisture and elevated CAPE values hover near this area, in a storm-relative sense. 700-500 lapse rates have been less than ideal, simply because frontal inversion now exists between those levels in many instances. However, model solutions do suggest substantial elevated CAPE values above the frontal zone, even though many of those parcels originate from 600-625 mb. Example from the 12Z/30 GFS 18Z solutions include 187 J/kg of CAPE at CQB for a parcel originating at 600 mb; this pattern diminishes at CQB, but persists at 00Z/01. These ingredients for elevated instability, with ample moisture and significant forcing progress across NE OK and into SW MO by 06Z/01, into the C75 region of IL by 12Z/01, and into the LP of MI by noon tomorrow.

Convective snow anticipated.

Appendix B

The following is the original TSSN forecast discussion written by *ROCS*

forecasters for 1800 UTC 19 January 2007 through 20 January 2007:

Day 1 - Forecast valid from 1800 UTC 19 January to 1800 UTC 20 January 2007

Still a bit of uncertainty with the exact track of our next system. Models seem to have dropped the forecasted path southward threatening the Southern and Central Plains once again with frozen precipitation. Main guidance for this forecast was taken from the GFS/WRF. Currently, 500mb closed low is located over the Baja Peninsula and already bringing snow and rain to portions of New Mexico and Texas. Once this system enters the main jet core in the southern plains, it is progged to spread into the central US by 18Z on the 20th bringing with it the chance of additional snowfall. Ample moisture coupled with strong forcing and freezing temperatures develop over Northern Texas and Southern Oklahoma by late day 1. Strong vorticity max and impressive vertical velocities accompany the main area of forcing adding additional lift and spin to the system. Weak frontogenesis couplets are also present across central Texas and into Southern Oklahoma. Soundings from northern Texas and Southern Oklahoma show temperature profiles within the desired 0 C to -10 C temp range for lightning production with saturated profiles and strong omega (-16 ub/s) values. Cross sections from HHF to LBF in northern TX reveal a well saturated atmosphere with regions of elevated (700-500 mb) CSI surrounded by additional CI and PI. Convective instability spills over into day 2 as the dynamic closed low continues to track E-NE. Lapse rates in both plan view and soundings are not very strong with highest values reaching to 5.8 C/km, which implies this system may not have the dynamics needed for a lightning producer. However, once the system is influenced by the low level jet pumping additional moisture in from the Gulf, and with all the other necessary elements present in this system, some lightning activity in the cold air is possible.

Convective snow anticipated.

Appendix C

The following is the original TSSN forecast discussion written by *ROCS*

forecasters for 1800 UTC 12 February 2007 through 13 February 2007:

Day 1 - Forecast valid from 1800 UTC 12 February to 1800 UTC 13 February 2007

Satellite imagery this morning shows thick cloud deck set up over portions of Texas, Kansas, Oklahoma, and Missouri associated with surface low pressure system and 500mb short wave. Moisture is streaming in from the southwest as cyclone is intensifying over the southern Plains. Currently, only liquid precipitation is falling across Texas and Oklahoma, as surface temps are well above freezing. A blend of GFS/NAM/WRF was used for this forecast discussion and indicates a large area of moisture across the central US. Limited forcing is present with this system, but vertical velocities over southern Missouri and Arkansas into Illinois, Indiana, and Ohio exceed -10 ubars/sec by 00Z Tues. 800mb frontogenesis shows a couplet develop over Oklahoma and northern Texas by 06Z Tues, spreading into southwest Missouri by 12Z, adding additional forcing to the area. These dynamics , however, are all confined to the warm sector of the system with the 5400 thickness gradient extending from Kansas through northern Missouri, Illinois, Indiana, and Ohio. The majority of instability for this system also seems to remain confined to the southern portion of this system where rain will be the only type of precipitation. A few pockets of moisture with adequate forcing are present in IA between 06 - 12Z Tues, but a closer look at soundings in the area indicate weak vertical velocities (less than 5 ubars/sec) and lapse rates of only 4.5 C/km.

No convective snow anticipated.

References

Banacos, P.C., 2003: Short Range Prediction of Banded Precipitation Associated with Deformation of Frontogenetic Forcing. Preprints, *10th Conf. On Mesoscale Processes*, Portland, OR, Amer. Meteor. Soc., CD-ROM, P1.7.

Crowe, C., P. S. Market, B. Pettegrew, C. Melick, and J. Podzimek, 2006: An Investigation of thundersnow and deep snow accumulations. *Geophys. Res. Lett.*, **33**, L24812, doi:10.1029/2006GL028214.

Johns, R.H., and C.A. Doswell, 1992: Severe Local Storms Forecasting. *Wea. Forecasting*, **7**, 588–612.

Market, P.S., C.E. Halcomb, and R.L. Ebert, 2002: A Climatology of Thundersnow Events Over the Contiguous United States. *Wea. Forecasting*, **17**, 1290–1295.

Market, P. S., A. M. Oravetz, D. Gaede, E. Bookbinder, R. Ebert, and C. Melick, 2004: Upper air constant pressure composites of Midwestern thundersnow events. *20th Conference on Weather Analysis and Forecasting*, Amer. Meteor. Soc., Seattle, WA.

Market, P. S., A. M. Oravetz, D. Gaede, E. Bookbinder, A. R. Lupo, C. J. Melick, L. L. Smith, R. Thomas, R. Redburn, B. P. Pettegrew, and A. E. Becker, 2006: Proximity soundings of thundersnow in the central United States. J. *Geophys. Res.*, **111**, D19208, doi:10.1029/2006JD007061.

Market, P.S., and A. E. Becker, 2009: A study of lightning flashes attending periods of banded snowfall. *Geophys. Res. Lett.*, in press. Moore, J.T., and T.E. Lambert, 1993: The Use of Equivalent Potential Vorticity to Diagnose Regions of Conditional Symmetric Instability. *Wea. Forecasting*, **8**, 301–308.

Nicosia, D.J., and R.H. Grumm, 1999: Mesoscale Band Formation in Three Major Northeastern United States Snowstorms. *Wea. Forecasting*, **14**, 346–368.

Novac, D. R., et al., 2003: An Observational Study of Cold Season Mesoscale Band Formation in the Northeast United States. *31st International Conference on Radar Meteorology,* Seattle, WA

O'Hara, B.F., M.L. Kaplan, and S.J. Underwood, 2009: Synoptic Climatological Analyses of Extreme Snowfalls in the Sierra Nevada. *Wea. Forecasting*, **24**, 1610–1624.

Pettersen, S., 1956: *Weather Analysis and Forecasting, Vol. 1.* New York, McGraw-Hill Book Company, 201-205 pp.

Saucier, W.J., 1955: *Principles of Meteorological Analysis.* Chicago, IL, The University of Chicago Press, 270-271 pp.

Schultz, D.M., and P.N. Schumacher, 1999: The Use and Misuse of Conditional Symmetric Instability. ***Mon. Wea. Rev.***, **127**, 2709–2732.

Schultz, D.M., P.N. Schumacher, and C.A. Doswell, 2000: The Intricacies of Instabilities. ***Mon. Wea. Rev.***, **128**, 4143–4148.

Sherwood, S.C., 2000: On Moist Instability. ***Mon. Wea. Rev.***, **128**, 4139–4142.

van den Broeke, M. S., D. M. Schultz, R. H. Johns, J. S. Evans, and J. E. Hales, 2005: Cloud-to- ground lightning production in strongly forced, low-instability convective lines associated with damaging wind. ***Wea. Forecasting***, **20**: 517–530.

Wilks, D.S., 2006*: Statistical Methods in the Atmospheric Sciences, Second Edition.* Burlington, MA, Elsevier Academic Press. 255-265 pp.